NATIONAL TECHNICAL UNIVERSITY OF ATHENS

SCHOOL OF NAVAL ARCHITECTURE AND MARINE ENGINEERING

DIVISION OF SHIP DESING AND MARITIME TRANSPORT

DIPLOMA THESIS

GEORGIA DOUSIA

Numerical Analysis of Parametric Roll Resonance of a Containership Sailing in Nonlinear, Longitudinal Seas

Supervisor: K. J. Spyrou, Professor NTUA

ACKNOWLEDGMENTS

The present thesis is the final milestone of my studies in the School of Naval Architecture and Marine Engineering of the National Technical University of Athens (NTUA). I would like to thank all my colleagues and professors, with whom I shared all these years. First of all, I would like to thank my family for their great support throughout my studies all these years, and for all their efforts and sacrifices they put into, so I could become a better person. Furthermore, I would like to offer my sincerest gratitude to my supervisor, Professor K.J. Spyrou. I would like to thank him for giving me the opportunity and the motivation to occupy with such an interesting subject, for the development of an ideal collaboration, for his valuable contribution to the thesis and for all his advices. Last but not least, I would like to thank doctoral student Ioannis Kontolefas for his great assistance in the accomplishment of the current thesis; it is fact that without his contribution, this thesis would not even present the half of the present content.

PREFACE

Parametric roll or “autoparametrically excited roll” is one of the major stability issues on large containerships. It is the phenomenon of substantial roll amplitude development, when the vessel is sailing in following or head seas. Even though hazard for capsizing exists mainly to smaller ships, such as fishing vessels, the economic consequences of cargo loss and damage of large containerships are extremely harmful to ship owners and the market in general.

As a parametric resonance phenomenon, parametric roll is characterized by a periodical alteration of one of its characteristics, in our case the restoring. As containerships have tended in the last twenty years to become larger, the need for maintaining low fuel consumption has led to the design of thinner hulls, with bow and stern flare sections. However, new containerships are optimized for a lower speed and their beam has become larger. In general, containerships are characterized by wide waterplane when the wave though is amidships, and respectively narrower when the ship is located in the wave crest. Since the waterplane area is directly connected to the transverse stability of the ship, a phenomenon of stability gain when the ship is in the wave trough and stability loss when it is positioned in the wave crest occurs.

The purpose of the present thesis is the construction of stability charts for parametric roll resonance of a containership sailing in longitudinal (head or following), regular and irregular seas. The investigation is focused on three layers: the nonlinearity of the waves, the influence of ship’s forward speed and the effect of the loading condition. A single-degree of freedom in roll with linear damping, characterized by an exact variation of the restoring has been used for the calculations. The stability charts are similar to Mathieu’s Ince-Strutt diagrams. Therefore, the horizontal axis is a function of the ship’s forward speed and the vertical axis is related to the wave steepness.

At first, numerical calculations were performed, which can provide the local value of metacentric height while the ship passes through each position on the wave. After the calculations of the variation of the metacentric height have been completed, numerical simulation is performed, by solving the differential equation of roll motion, for several values of ship’s forward speed and wave steepness. Finally, stability charts are produced, where the instability regions correspond to the roll amplitudes exceeding a given threshold value, within a given number of wave cycles.

In particular, stability charts for four different loading conditions are created. The selected conditions correspond to the design as well as the scantling draft. In addition, the values of the initial metacentric height cover the whole range of all loading cases. For the three out of four conditions, comparison of ship tendency for parametric rolling inharmonic and in nonlinear waves is realized. Furthermore, charts with the instability regions separated into regions of ship’s forward speed are constructed, for all loading cases and for both regular and irregular seas. These charts can provide valuable information on the proper speed regions for the prevention of parametric roll resonance, according to the selected loading case and whether regular or irregular seas are considered .Given the fact that

nowadays containership are designed with a Slow Steaming service speed, these charts can indicate in which cases Slow Steaming speeds should be preferred to higher speeds, and in converse. Consequently, these charts can be also used as a guide for speed on board, apart from tools of early detection of parametric roll resonance.

ΠΕΡΙΛΗΨΗ

Ο παραμετρικός διατοιχισμός αποτελεί ένα από τα κυρίαρχα προβλήματα ευστάθειας που αφορούν στα μεγάλα containerships. Αποτελεί το φαινόμενο της προοδευτικής ανάπτυξης μεγάλων εγκάρσιων κλίσεων, καθώς το πλοίο ταξιδεύει σε ακολουθούντες (πρυμναίους) κυματισμούς. Παρόλο που ο κίνδυνος για ανατροπή υφίσταται κυρίως σε μικρότερα πλοία, όπως τ' αλιευτικά, πιθανή απώλεια ή/και καταστροφή φορτίου στα μεγάλα containerships θα έχει ισχυρές οικονομικές συνέπειες τόσο στην πλοιοκτήτρια εταιρία όσο και στην αγορά της ναυτιλίας γενικότερα.

Ως ένα φαινόμενο παραμετρικής αστάθειας, ο παραμετρικός διατοιχισμός χαρακτηρίζεται από την περιοδική μεταβολή ενός βασικού χαρακτηριστικού του: της ικανότητας επαναφοράς του. Με την πάροδο του χρόνου, τα containerships γίνονται όλο και μεγαλύτερα σε μέγεθος. Προκειμένου να μην αυξηθεί η κατανάλωση του καυσίμου, σχεδιάζονται λεπτότερες γάστρες, με νομείς στην πλώρη και στην πρύμνη που εμφανίζουν απότομη κλίση (flare). Αυτό έχει ως αποτέλεσμα η ίσαλος επιφάνεια να γίνεται στενότερη όταν το μέσο του πλοίου βρίσκεται στην κορυφή του κύματος, και πιο πλατιά όταν βρίσκεται στην κοιλάδα. Η επιφάνεια της ισάλου, όμως, συμβάλλει καθοριστικά στην εγκάρσια ευστάθεια του πλοίου. Συνεπώς, παρατηρείται το φαινόμενο της αύξησης της ευστάθειας όταν η κοιλάδα του κύματος διέρχεται από το μέσο νομέα του πλοίου, και της μείωσης της ευστάθειας όταν το πλοίο διέρχεται από την κορυφή του κύματος.

Ο στόχος της παρούσης εργασίας είναι η κατασκευή διαγραμμάτων ευστάθειας για τον παραμετρικό διατοιχισμό ενός πλοίου μεταφοράς εμπορευματοκιβωτίων, που ταξιδεύει σε διαμήκεις (ακολουθούντες ή πρυμναίους), μη γραμμικούς κυματισμούς. Η μελέτη της παραμετρικής αστάθειας επικεντρώνεται σε τρία σημεία: στη μη γραμμικότητα των κυματισμών, στην επίδραση της πρόσω ταχύτητας του πλοίου και τέλος, στο ρόλο που διαδραματίζει η εκάστοτε κατάσταση φόρτωσης. Το μοντέλο που χρησιμοποιήθηκε για τους υπολογισμούς είναι γραμμικό, ενός βαθμού ελευθερίας και με γραμμική απόσβεση. Το κύριο χαρακτηριστικό του είναι ότι περιέχει την ακριβή μεταβολή του όρου της επαναφοράς. Τα διαγράμματα ευστάθειας είναι παρόμοια με εκείνα του Mathieu. Ο οριζόντιος άξονας είναι συναρτήσει της ταχύτητας του πλοίου, ενώ ο κατακόρυφος είναι ανάλογος του ύψους του κύματος.

Αρχικά, δημιουργήθηκε ένας αριθμητικός κώδικας ο οποίος υπολογίζει την ακριβή τιμή του εγκάρσιου μετακεντρικού ύψους καθώς το πλοίο διατρέχει κάθε θέση πάνω στο κύμα. Μετά το πέρας των υπολογισμών που αφορούν στη μεταβολή του μετακεντρικού ύψους κατά μήκος του κύματος, γίνεται χρήση ενός επιπλέον αριθμητικού κώδικα, που κατασκευάστηκε επίσης στα πλαίσια της παρούσης εργασίας, προκειμένου να επιλυθεί αριθμητικά η γραμμική εξίσωση διατοιχισμού, για τις διάφορες ταχύτητες του πλοίου και για τα διάφορα ύψη κύματος. Τελικά, κατασκευάζονται τα διαγράμματα ευστάθειας, όπου με τον όρο αστάθεια εννοούμε την περιοχή όπου υπερβαίνεται μία δεδομένη οριακή τιμή εγκάρσιας κλίσης, για ένα δεδομένο αριθμό κύκλων κυμάτων.

Τελικά, κατασκευάζονται διαγράμματα ευστάθειας για τέσσερις διαφορετικές καταστάσεις φόρτωσης του υπό μελέτη πλοίου. Οι καταστάσεις έχουν επιλεγεί με τέτοιο

τρόπο, ώστε να αντιστοιχούν κάποιες στο βύθισμα σχεδίασης και κάποιες στο «scantling draft». Επίσης, τα αρχικά μετακεντρικά ύψη καλύπτουν όλο το εύρος των καταστάσεων φόρτωσης. Για τις τρεις από τις τέσσερις καταστάσεις, πραγματοποιείται σύγκριση ανάμεσα στους γραμμικούς και στους μη γραμμικούς κυματισμούς. Επιπλέον, δημιουργούνται διαγράμματα ευστάθειας που περιλαμβάνουν και τις διάφορες περιοχές των ταχυτήτων του πλοίου. Τα διαγράμματα αυτά παρέχουν σημαντικές πληροφορίες σχετικά με το ποία περιοχή ταχυτήτων δρα θετικά στην αποφυγή της παραμετρικής αστάθειας, ανάλογα με το αν οι κυματισμοί είναι γραμμικοί ή όχι. Είναι γεγονός ότι τα τελευταία χρόνια επικρατεί η τάση σχεδιασμού πλοίων containershipγια χαμηλότερες ταχύτητες («slow steaming»). Συνεπώς, τα διαγράμματα ευστάθειας με περιοχές ταχυτήτων μπορούν να αποτελέσουν μία ένδειξη ως προς το ποιο εύρος ταχυτήτων θα πρέπει να προτιμάται, ανάλογα με την κατάσταση φόρτωσης του πλοίου και το είδος των κυματισμών. Κατά συνέπεια, εκτός από εργαλεία πρόβλεψης της εμφάνισης της παραμετρικής αστάθειας, τα διαγράμματα αυτά μπορούν να χρησιμοποιηθούν ως οδηγία για την επιλογή της κατάλληλης ταχύτητας εν πλω.

CONTENTS

1. INTRODUCTION

"Masters who do not identify the 'right conditions' for parametric roll have been in for a huge surprise, with consequent loss of cargo and danger to the ship and crew'', says Knut A. Dohlie, DNV's business director for container ships, at the DNV Greater China Technical Committee meeting in 2008 [38]. Although parametric roll has been well known to the naval architecture society for more than half and century, it was not considered as a top priority stability issue until the 1990s. The infamous APL China casualty in 1998 was the event which urged reconsideration of the perspective that parametric roll concerns only low freeboard ships of low marginal stability, such as fishing vessels [24]. Smaller vessels experiencing parametric roll may be more prone to capsizing than larger ships, such as containerships; but even 'non-capsizal' instabilities can lead to significant cargo loss and damage of construction elements of the ship [29]. Such phenomena can induce severe economic loss to the ship owners and damage to the market in general. An example of parametric roll behavior is shown in figure 1.1.

Figure 1.1: Container ship under the influence of parametric roll [36]

As containerships tend to become even larger with time in order to achieve economies of scale and respond to conditions of the market, parametric roll requires more attention. For many years, as these ships increased in size they maintained the level of service speed as high as it has been since the seventies, where ships had a payload of around 2000 containers (this trend was reversed recently due to the introduction of the Energy Efficiency Design Index by the International Maritime Organization). Nowadays, the payload reaches 15000 and well above it. To achieve a relatively high speed, the shape of the hull needed to become much thinner, so that the fuel consumption is not too high [32]. This "builds-in" some characteristics that are fundamental for the development of parametric roll resonance, as we will analyze later. At first, the length of the ship is significantly increased, comparable to the length of big waves encountered in the Pacific and the North Atlantic Ocean. Secondly, the bow and stern shapes are much thinner, including flare sections, while

the midship section is a fixed U-shaped cross section [32]. The waterplane area becomes more prone to gain or loss when the ship travels in waves.

Parametric rolling is the phenomenon of development of substantial roll amplitude, while a vessel is sailing in following or head seas. It belongs to the family of parametric resonance phenomena that occur in systems experiencing dynamic alteration of at least one of its key dynamic characteristics [16]. It has been proven that when a ship is sailing in longitudinal waves, its transverse stability changes periodically with time. In particular, stability increases when the ship is located in the wave trough, while it decreases when the ship is positioned in the wave crest. This response is intensified for the containerships where, the hull shape of the bow and stern area results to the waterplane area becoming narrower when the wave crest is amidships and respectively wider when the wave trough is amidships.

As already mentioned, the APL China casualty was the turning point for the researchers to start investigating thoroughly the parametric roll resonance for large containerships. In [1]SNAME's annual meeting in 2001, France et al. [13] presented the conditions under which the incident took place. While the post-Panamax, C11 class containership was travelling form Kaohsiung to Seattle, it encountered a violent storm in the North Pacific Ocean. During the encounter with the storm, the master reduced the speed. The roll angles that were developed reached up to forty degrees and the master of the ship claimed that the ship was completely out of control. The one third of the on-deck containers along with their cargoes was lost, while another one third, with their cargoes, was in a situation of heavy damage. Even at the early stage of the investigation of the accident, the lawyers claimed that the loss of the cargo was more than fifty million dollars, an amount that is higher than the value of the vessel, fact which established the APL China casualty as the largest in history until then. Images of damage to vessel and cargo are shown in figure 1.2.

Figure 1.2: The APL China casualty [37].

From studies accomplished in both theoretical and experimental level by Dallinga [29], Luth [30] and France et. al [13], parametric roll develops when combination of the four following factors exists:

1. The wave encounter period is equal to almost twice the natural rolling period of the ship

[1] SNAME: Society of Naval Architecture and Marine Engineering.

2. The wave height exceeds a threshold value
3. The roll damping is of low magnitude [21]

Another well-known casualty with possible connection with parametric rolling is that of the *Maersk Carolina* containership. In 2003, the Panamax vessel came across a storm in the North Atlantic Ocean, where it experienced gale-force winds and seas [7]. After the influence of an intense rolling and pitching disturbance, large roll angles upwards of 47 degrees started to develop quickly and unpredictably. The result of this incident was the loss of 133 containers and the serious water damage of 50 other that managed to be maintained on board. The cargo damage amounts up to 4 million dollars, while structural elements of the ship needed to be repaired.

Figure 1.3: The Maersk Carolina casualty [37].

The most common method for the prediction of parametric roll resonance is Mathieu's Ince-Strutt diagrams, or else Stability Charts. They are based on a single-degree of freedom model, with linear damping as well as linear restoring term. This model is often applied for the case of regular, harmonic waves. However, even when the encounter waves are harmonic, the variation of the metacentric height should not be considered as harmonic too, but rather, as just periodic. The assumption of linear damping may contribute to the overestimation of the resonance [30]. In general, the nonlinearity in damping seems to be less significant than the nonlinearity in restoring [14]. Numerous efforts for a more realistic approach to the variation of the metacentric height, most of them through polynomial fittings or Fourier series, have been realized. In addition, the sea waves are far from linear. They are better described through nonlinear wave forms and even better through stochastic processes of wave groups. Stability charts that are based on an exact calculation of the metacentric height that takes into full consideration the hull geometry, while considering irregular wave forms, would compose a strong tool for the prediction of parametric roll resonance. In addition, if the influence of ship's forward speed is also taken into consideration, these charts could be used also as an operational guide on board, apart from their use as early prediction tools.

2. LITERATURE REVIEW

2.1 BACKGROUND

As said earlier, parametric rolling belongs to the family of parametric resonance phenomena. These can develop in a system whose one or more coefficients change periodically with time. Faraday [6, 11] was the first to observe the parametric resonance phenomenon, followed by Melde. Parametric resonance is described by a mathematical model given by Mathieu [16].

It seems that the phenomenon of parametric resonance in ships was first detected by William Froude [15]. In 1863, the famous naval architect stated that a ship sailing in longitudinal waves with frequency of oscillation in heave coupling with pitch motion being twice its natural rolling frequency, presents unfavorable seakeeping behavior, which can cause the vessel to experience exciting large roll angles [16,24]. Research for parametric rolling was first accomplished in Germany in the late 1930s [24]. At first, in 1938 Krempf made the significant observation that the stability of a ship is decreased when the wave crest is amidships, while it is decreased when the ship is located in the wave trough. [35]. In addition, several facts of capsizing of a number of small ships, such as fishing vessels and coasters in following waves indicated the need for further investigation [24]. Therefore, research was accomplished in both theoretical and experimental level, with model experiments realized by Heckscher and Graff in 1941[35].

In 1950s, professors Grim and Kerwin observed that the periodical alteration of the metacentric height while the ship is sailing in head or following seas, results to the differential roll equation becoming of Mathieu type [35]. Consequently, Kerwin [19] tried to examine the response of a ship in regular seas, using a single-degree of freedom model with the constraint of fore-aft symmetry of the hull [16]. The results from both analytical and experimental process showed that roll angles needed an incredibly large amount of time to increase significantly. Therefore, Kerwin presumed that parametric roll was not a practical issue for linear waves. The initial conclusion, however, that the roll equation is of Mathieu type is based on the consideration that regular encounter waves lead to a harmonic variation of the metacentric height. This assumption is merely approximating, whereas the variation of the restoring should be considered as simply periodical [35].

Subsequently, the interest of the scientific community was concentrated on the expansion of Kerwin's single-degree of freedom model to a more complex one, since the ship usually experiences a coupling between roll and heave or pitch motion. In 1959Paulling and Rosenberg [23] proposed a nonlinear model with three degrees of freedom andthey carried out experiments, proving that parametric roll was actually a real, practical issue on ship stability [16].Twenty years later, Blocki [4] examined the probability of prediction of parametric resonance development, for both heave-roll and pitch-roll coupling and for a specific loading case and type of wave [16].

2.2. MORE RECENT STUDIES

In the last fifteen years, the phenomenon of parametric roll has been extensively studied by many scientists and organizations (classification societies etc). In 2004, ABS[2] presented a technical paper where the background of *"Guide for the Assessment of Parametric Roll Resonance in the Design of Container Carriers"* was discussed [28]. In the paper, susceptibility criteria with respect to the hazard of the development of parametric roll; and calculation methods for the roll amplitudes in longitudinal waves, were proposed. The considered model for the establishment of susceptibility criteria was a single degree of freedom equation written in the form of Mathieu's equation and the variation of the metacentric height with time was assumed as sinusoidal. Ince–Strutt diagrams, as obtained through the solution of the Mathieu's equation, are also presented in the paper. In addition, the significance, concerning the susceptibility criteria, of ship's forward speed is discussed. It was generally believed that a ship entering heavy-weathered conditions should reduce its forward speed. It seems through this analysis, however, that this perspective does not always benefit large containerships, in contrary perhaps to the case of smaller vessels.

As already mentioned, parametric roll resonance results from the periodic alteration of the ship's stability on waves. Belenky and Bassler [2] have presented a quite simple and practical method for early-stage ship design for the assessment of stability variation in irregular seas. The method is taking into account the hull geometry of the ship and therefore it can be used for any type of vessel. The free surface elevation is considered as a stochastic sinusoidal process and the for the calculation of stability while the ship passes the waves, the metacentric height is written as a function of the position of the wave crest. The possibility of the ship experiencing stability failure is defined by the ratio between the average time of the calculated GM being below critical level and the natural rolling period of the ship.

In 2005, Spyrou [29] proposed design criteria for the prevention of parametric roll, for a deterministic as well as for a probabilistic environment (the latter based on consideration of wave groups). As far as it concerns the deterministic approach, the amplitude of the metacentric height variation is scaled to the ship's initial one in still water, while the model describing the roll motion is based on Mathieu's equation with damping. A few years earlier, Spyrou [30] had investigated both analytically and numerically the parametrically excited roll with presence of extreme alteration of stability between the wave crest and the wave trough. The paper presents instability charts in terms of transient motions. Here, an effort for a realistic calculation of the restoring was attempted, through polynomial approximations of the GZ curve. In a more recent study, Spyrou et.al [31] examined the parametric rolling behavior of a post-panamax containership, attempting to evaluate Mathieu's system by continuation analysis. At first, analytical study on parametric roll was accomplished with application of a formula provided by ITTC in [18] that has been deduced by the method of harmonic balance. Then, a containership model was introduced into the software MaxSurf, where exact GZ curves were calculated, for several positions of the ship on a regular wave, under the condition of vertical equilibrium. The GZ variation was then

[2]American Bureau of Shipping

fitted by a three-parameter procedure, based on an approximation by Scanferla [26]. In addition, numerical simulations by the numerical time-domain panel code SWAN2 were realized. Finally, stability charts that represent the parametric roll boundaries are created, for the analytical method, the continuation and the numerical analysis.

An effort for a realistic approach to the restoring term can also be seen in a paper presented by Umeda et. al [33], where the GZ curve is described as a nonlinear function of wave steepness in analytical, geometrical and experimental level. Here, stability charts of parametric roll resonance are constructed through application of the Poincare mapping technique. In the same year, Bulian [5] presented an investigation of parametric roll in both regular and irregular seas, where the environment of irregular sea is described as a stochastic process, developing a nonlinear mathematical model were the influence of heave and pitch on roll motion is modeled as a parametric excitation. The nonlinear variation of GZ curve is given as an approximating expression in terms of parameters that depend on wave characteristics and the considered relation between pitch, heave and wave position. Apart from analytical study, numerical simulations and model tests were also materialized.

Another numerical analysis of parametric roll of a container vessel in irregular seas was realized by Hong et. al [25]. Several numerical simulations were carried out order to determine critical wave heights and periods for susceptibility to parametric roll. Spanos and Papanikolaou accomplished a benchmark study in order to evaluate the prediction of parametric roll of a containership by various numerical methods [27]. For the simulation of ship hydrodynamics within the potential theory, either a strip method or a panel method was applied. The numerical codes were all nonlinear time-domain codes but they differed in several respects such as in damping, in the degrees of freedom, in wave profiles and in the approximation of the GZ curve. Quite recently, an interesting investigation on parametric roll of container ships in head, regular seas was accomplished by Moideen et. al [10]. The roll equation is suggested here as a Hill's equation, rather than a Mathieu type, since there is an effort to avoid the common assumption of fully harmonic variation of the metacentric height. At first, the paper presents Ince-Strutt diagrams based on the Mathieu equation, considering a sinusoidal variation of GM. Later, it proceeds to an approximation of the stability change based on the vessel's hull, through several values of GM that are obtained from standard hydrostatic software, while the ship passes one wavelength. A cosine fitting with shaft is applied on these values, since the simple cosine fit is not a proper representation of the GM variation [2, 31]. Nevertheless, the change of GM is more accurately obtained through Fourier series, in order to be introduced later to Hill's equation. Finally, Hill's stability charts are created, with the effect of both linear and nonlinear damping being taken into consideration. A significant aspect of this study is the investigation of the influence of ship's forward speed in the development of parametric resonance. Therefore, stability charts that represent the stable and unstable regions of the ship's response to parametric roll, while the speed of the ship varies, are also included.

3. THESIS OUTLINE - CONTRIBUTIONS

The purpose of this thesis is the construction of stability charts with respect to parametric roll resonance of a containership for linear and for higher orders Stokes waves (up to 5^{th} order). In the current study, both following and head seas are taken into consideration, while the waves are described by Stokes wave theory, for orders ranging from one up to five. The mathematical model for the description of the wave form is given by Fenton [12] and it is presented, along with a brief theoretical review of surface gravity waves, in chapter 4. A theoretical review of parametric roll instability in longitudinal waves is presented in chapter 5. The mathematical model that is used is single-degree of freedom. The main novelty of the current methodology lies on the consideration of the restoring term. In contrary to earlier studies, the variation of the metacentric height is neither described by a harmonic function nor by an approximating polynomial. A numerical calculation method taking into consideration the detailed hull geometry is created, which can provide the value of the metacentric height for every position of the ship on the encounter wave. Of course, several studies exist that include a realistic GM alteration, as provided by the introduction of ship hull into design programs such as MaxSurf. Nevertheless, these have the constraint of sinusoidal or trochoidal wave form and therefore, they cannot be applied on arbitrary wave forms. It seems then, that combination of exact calculation of the restoring and nonlinear encounter waves is not an easy task.

The methodology of exact GM calculation is presented in chapter 6. The procedure for finding ship vertical equilibrium state on a wave, as long as the method for the calculation of the local drafts of the sections in each equilibrium state, are provided in the thesis of Kontolefas[34]. Finally, the variation of GM is obtained as pairs of (x, GM_x), where x and GM_x are respectively the position amidships on the wave and the corresponding GM. In the same chapter, the verification of the GM calculation methodology is presented, by comparing the GM variations as provided by the numerical simulation to those obtained by the software MaxSurf, for the case of regular waves.

For the construction of stability charts, a numerical code that solves repeatedly the differential roll equation is created. The stability charts are similar to Mathieu's Ince-Strutt diagrams[3], with the fundamental difference that the equation of motion model is not a Mathieu type, but includes the real variation of the restoring, as already discussed. The methodology on which the construction of the stability charts is based is presented analytically in chapter 7. It is important to highlight that the variation of GM as pairs or (x, GM_x) is not fitted to a polynomial or series.

In chapter 8, stability charts for regular and irregular seas and for four different loading conditions of the containership model are presented. In addition, emphasis is given on the influence of ship's forward speed in the limits of unstable regions and stability charts that include also regions of speed range are created. Apart from the realistic calculation of the

[3] Mathieu's mathematical model and Ince-Strutt diagrams can be seen in chapter 4.

restoring term in both regular and irregular seas, the thesis contributes also to the evaluation of when should the vessel increase or decrease its forward speed, in order to avoid parametric roll. In addition, the investigation in four different loading conditions gives

a more complete perspective to the response of the containership model to parametric roll. That is mainly because the conditions selected correspond both the design and the scantling draft, covering the whole range of values of the initial metacentric height. Last but not least, a comparison between the unstable regions when the same initial metacentric height but two different drafts have been considered is presented. This allows us to evaluate whether change of the draft will have a substantial influence on the stability charts. The final conclusions of the current thesis, as well as recommendations on future work, are presented in final chapter 9.

4. SURFACE GRAVITY WAVES

4.1 INTRODUCTION

The sea environment is a place where variable forms of waves evolve simultaneously, with many of them being in conjugation. The most familiar form of wave motions is the surface gravity waves, which owe their existence to the large difference of density between water and overlying air [1]. Consequently, we can examine gravity waves on the surface of a body of water without taking into consideration that either the surface of the water or the air above is satisfied.

At first, we will analyze the most simple wave form, i.e. the linear waves. In this case, the mathematical problem that describes the motion of the surface, and which will be constructed in the chapter 4.2.1 by the appropriate equations and boundary conditions, is fully linearized. Apart from the linearization, though, there are other methods that provide solution to the mathematical problem discussed. One of them is the Stokes wave theory, which will be presented in the chapter 4.3. This theory will be displayed through Fenton's mathematical model which is based on distribution series that also define the order of the model. In addition, we mention that there are also two famous wavelet theories, such as the Cnoidal waves and the Fourier approximation methods.

4.2 LINEAR (AIRY) WAVES

The theory of linear or else airy waves was first introduced by George Biddell Airy in the 19thcentury and it gives a linearized description of the propagation of surface gravity waves [8]. A wave is specified by its amplitude a, its wavelength λ and its period T, as shown in figure 4.1.

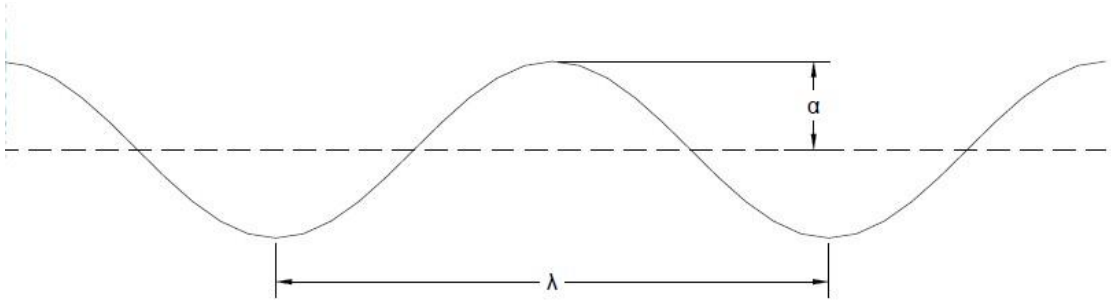

Figure 4.1: Characteristics of the cosine wave

The free surface elevation of a regular wave is a two variable (x, t) harmonic function, such as:

$$\eta(x,t) = a\cos(kx - \omega t) \tag{4.1}$$

Where,

$a = \frac{H}{2}$,with H the wave height

$k = \frac{2\pi}{\lambda}$,known as the wavenumber

$\omega = \frac{2\pi}{T}$, the angular frequency.

We also define the wave speed or wave celerity as: $c = \frac{\lambda}{T} = \frac{\omega}{k}$

4.2.1 EQUATIONS AND BOUNDARY CONDITIONS

In order to define the motion of the surface, we need first to formulate the mathematical problem. Therefore, we are going to introduce the necessary assumptions respecting the fluid, as long as the boundary conditions.

At first, we consider waves that travel in a channel with parallel walls and horizontal bottom. The latter is identical to the layer z=-d and we assume that there are no variations in the wave form across the channel. (Figure 4.2)

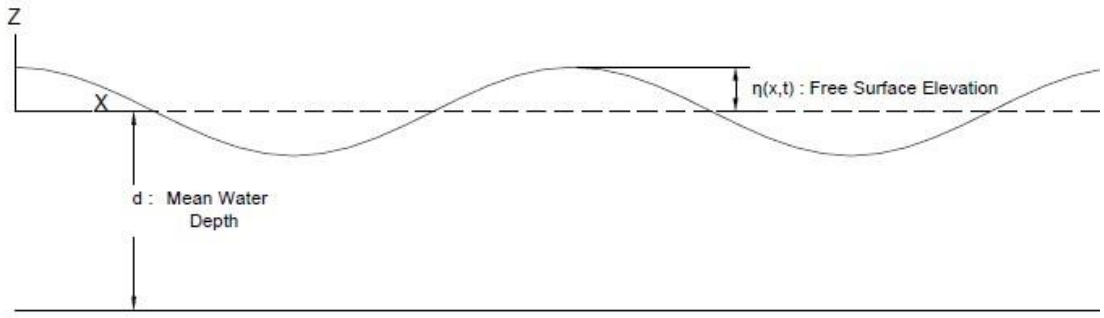

Figure 4.2: Waves along the channel

It is true that water is a hard to compress fluid, and for this analysis, we will consider it *incompressible*. In an incompressible fluid, the velocity v= (u, v, w) at each point satisfies the following equation,

$$\frac{\partial u}{\partial x} + \frac{\partial v}{\partial y} + \frac{\partial w}{\partial z} = 0 \tag{4.2}$$

which is also known as the *equation of continuity*[17].

Because we do not take into account the possible variations across the channel, the y-component of the velocity is considered zero and the equation (4.2) becomes,

$$\frac{\partial u}{\partial x}+\frac{\partial w}{\partial z}=0 \tag{4.3}$$

We consider also the fluid as *irrotational* and the velocity can be expressed by the potential velocity as follows,

$$u=\frac{\partial \Phi}{\partial x}$$
$$v=\frac{\partial \Phi}{\partial y} \tag{4.4}$$
$$w=\frac{\partial \Phi}{\partial z}$$

We now introduce the above expression of the velocity potential to the continuity equation and we obtain,

$$\frac{\partial^2 \Phi}{\partial x^2}+\frac{\partial^2 \Phi}{\partial z^2}=0 \tag{4.5}$$

which is the famous *Laplace Equation*.

Afterwards, we are going to introduce the boundary conditions. The first one relates to the fact that the bottom of the channel is not permeable to water, and therefore the vertical water velocity must be always zero.

$$w(x,z=-d,t)=\frac{\partial \Phi}{\partial z}(x,z=-d,t)=0 \tag{4.6}$$

The other boundary conditions are with respect to the free surface elevation. At first, the fluid molecules that are part of the surface should remain always at the surface. This is the *kinematic boundary condition,* described as follows:

$$\frac{\partial \eta}{\partial t}+u\frac{\partial u}{\partial x}=w \tag{4.7}$$

The last boundary condition has to do with the force on the surface and therefore is called the *dynamic boundary condition*. At first, we will introduce the Bernoulli's Equation:

$$\frac{p}{\rho}+\ \frac{\partial \Phi}{\partial t}+\frac{1}{2}(\mathrm{u}^2+w^2)^2+g\ z=0 \tag{4.8}$$

Where ρ is the density of the fluid and g is the acceleration of gravity.

The condition that must be satisfied is that the pressure p at the surface must be equal to the constant-as we assume- atmospheric one. Finally, the Bernoulli's equation gives for the free surface:

$$\frac{\partial \Phi}{\partial t} + \frac{1}{2}(\mathrm{u}^2 + w^2)^2 + g\,\eta = 0 \tag{4.9}$$

The mathematical problem described in equations (4.5) to (4.9) is very difficult and does not accept a general analytical solution. However, the airy wave theory can linearize these equations, with the restriction of very small wave amplitudes in comparison to the wavelength.

4.2.2 LINEARIZATION

As it is mentioned in the previous chapter, in order to linearize the mathematical problem with respect to the motion of the surface, we need to consider the case of small amplitude gravity waves, so that α<<λ, i.e. α/λ<<1. Therefore, if we linearize the Laplace equation, the boundary condition corresponding to the bottom and the kinematic and dynamic boundary conditions that refer to the free surface, the new mathematical model is described as follows:

$$\frac{\partial^2 \Phi(x,z,t)}{\partial x^2} + \frac{\partial^2 \Phi(x,z,t)}{\partial z^2} = 0\,, \qquad -d \le z \le \eta \tag{4.10}$$

$$\frac{\partial \Phi}{\partial z}(x, z = -d, t) = 0 \tag{4.11}$$

$$\frac{\partial \eta}{\partial t}(x,t) = w(x,0,t) \tag{4.12}$$

$$\frac{\partial \Phi}{\partial t}(x,0,t) + gz + \frac{p}{\rho} = 0 \tag{4.13}$$

The solution of the system (4.10) to (4.13) is provided by the method of separation of variables. Consequently, we get the expression for the velocity potentialΦ,

$$\Phi(x,z,t) = \alpha \frac{g}{\omega} \frac{\cosh[k(z+d)]}{\cosh(k\,d)} \sin(k\,x - \omega t) \tag{4.14}$$

If we now insert this expression to the linearized Bernoulli's Equation (4.13), we obtain the relation for the pressure field,

$$p(x,z,t) = -\rho\,g\,z + \rho\,g \frac{H}{2} \frac{\cosh[(z+d)]}{\cosh(k\,d)} \cos(k\,x - \omega t) \tag{4.15}$$

The chapter of linear wave theory will be completed with the definition of the term *dispersion relation*. Generally, if a wave has a given value of frequency, then it has a certain wavelength-for a specific water depth. Consequently, concerning the airy waves where the

harmonic expression of free surface elevation is $\eta(x,t) = a\cos(kx - \omega t)$, the dispersion relation is given by

$$\omega^2 = g\, k \tanh(k\, d) \tag{4.16}$$

In addition, since the wave celerity is defined as $c = \frac{\omega}{\lambda}$, we obtain

$$c^2 = \frac{g}{k}\tanh(k\, d) \tag{4.17}$$

and if we introduce the definition of the wave number $k = \frac{2\pi}{\lambda}$,we get

$$c = \pm\sqrt{\frac{g\lambda}{2\pi}\tanh\left(\frac{2\pi\, d}{\lambda}\right)} \tag{4.18}$$

As shown in the equation above, the term $\tanh\left(\frac{2\pi\, d}{\lambda}\right)$ depends on whether the waves are in region of shallow or deep water, i.e. the dispersion relation is a function of the ratio λ/d (figure 4.3). Therefore, we consider the following cases:

Shallow water region: λ/d > 20

$$c = \pm\sqrt{g\, d} \tag{4.19}$$

Deep water region: λ/d<2

$$c = \pm\sqrt{\frac{g\lambda}{2\pi}} \tag{4.20}$$

Last, for the *intermediate water region: 2<λ/d<20,* the general expression (4.18) is used.

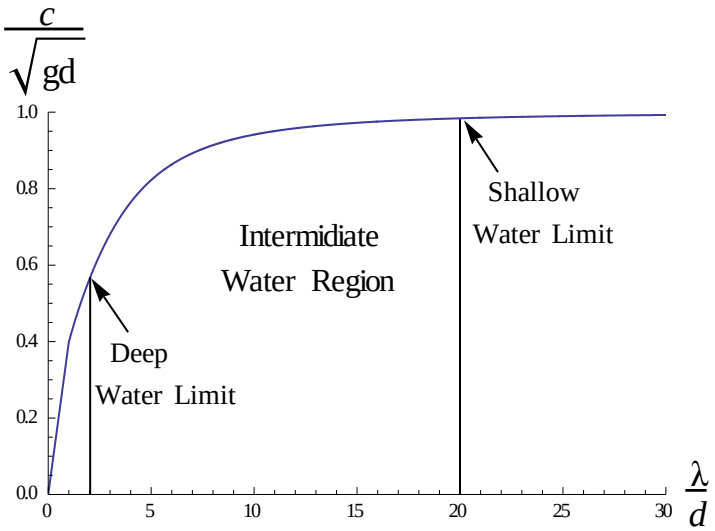

Figure 4.3: The wave speed of a surface gravity wave as a function of the ratio λ/d.

4.3 STOKES THEORY

Stokes assumed that the mathematical problem described in chapter (4.2.1) can be formulated with Fourier series with coefficients written as perturbation expansions in terms of the dimensionless parameter $\varepsilon = \frac{kH}{2}$ [7]. Fenton has recently presented a mathematical model of Stokes theory that preserves terms to fifth order [12].

At first, the wave celerity is provided by Stokes theory as the following relation:

$$c = \frac{1}{(k/g)^{1/2}}(C_0 + \varepsilon^2 C_2 + \varepsilon^4 C_4 + \cdots) \tag{4.21}$$

Here, the coefficients C_0, C_2 and C_4 depend on the dimensionless parameter *kd* and are given in table 4.1. At this point, we need to mention that the coefficient C_0 refers to the first and second order problem, while the coefficients C_2 and C_4 are considered with respect to the third and fifth order problem. The wave height-varying nature of the wave celerity is shown in figure 4.4.

$A_{11} = 1/\sinh(kd)$

$A_{22} = 3S^2/(2(1-S)^2)$

$A_{31} = (-4 - 20S + 10S^2 - 13S^3)/(8\sinh(kd)(1-S)^3))$

$A_{33} = (-2S^2 + 11S^3)/(8\sinh(kd)\,(1-S)^3)$

$A_{42} = (12S - 14S^2 - 264S^3 - 45S^4 - 13S^5)/(24(1-S)^5)$

$A_{44} = (10S^3 - 174S^4 + 291S^5 + 278S^6)/(48(3+2S)(1-S)^5)$

$A_{51} = (-1184 + 32S + 13232S^2 + 21712S^3 + 20940S^4 + 12554S^5 - 500S^6 - 3341S^7 - 670S^8)/(64\sinh(kd)\,(3+2S)(4+S)(1-S)^6)$

$A_{53} = (4S + 105S^2 + 198S^3 - 1376S^4 - 1302S^5 - 117S^6 - 58S^7)/(32\sinh(kd)\,(3+2S)(1-S)^6)$

$A_{55} = (-6S^3 + 272S^4 - 1552S^5 + 852S^6 + 2029S^7 + 430S^8)/(64\sinh(kd)(3+2S)(4+S)(1-S)^6)$

$B_{11} = 1$

$B_{22} = \coth(kd)\,(1+2S)/(2(1-S))$

$B_{31} = -3(1 + 3S + 3S^2 + 2S^3)/(8(1-S)^3)$

$B_{33} = -B_{31}$

$B_{42} = \coth(kd)\,(6 - 26S - 182S^2 - 204S^3 - 25S^4 + 26S^5)/(6(3+2S)(1-S)^4)$

$B_{44} = \coth(kd)\,(24 + 92S + 122S^2 + 66S^3 + 67S^4 + 34S^5)/(24(3+2S)(1-S)^4)$

$$B_{53} = 9(132 + 17S - 2216S^2 - 5897S^3 - 6292S^4 - 2687S^5 + 194S^6 + 467S^7 + 82S^8)/(128(3 + 2S)(4 + S)(1 - S)^6)$$

$$B_{55} = 5(300 + 1579S + 3176S^2 + 2949S^3 + 1188S^4 + 675S^5 + 1326S^6 + 827S^7 + 130S^8)/(384(3 + 2S)(4 + S)(1 - S)^6)$$

$$B_{51} = -(B_{53} + B_{55})$$

$$C_0 = (\tanh(kd))^{1/2}$$

$$C_2 = (\tanh(kd))^{1/2}(2 + 7S^2)(4(1 - S)^2)$$

$$C_4 = (\tanh(kd))^{1/2}(4 + 32S - 116S^2 - 400S^3 - 71S^4 + 146S^5)/(32(1 - S)^5)$$

$$E_2 = tanh(kd)(2 + 2S + 5S^2)/(4(1 - S)^2)$$

$$E_4 = tan\,h(kd)\,(8 + 12S - 152S^2 - 308S^3 - 42S^4 + 77S^5)/(32(1 - S)^5)$$

Table 4.1: Coefficients used in Stokes theory in terms of hyperbolic functions of kd, including S=sech2kd [7].

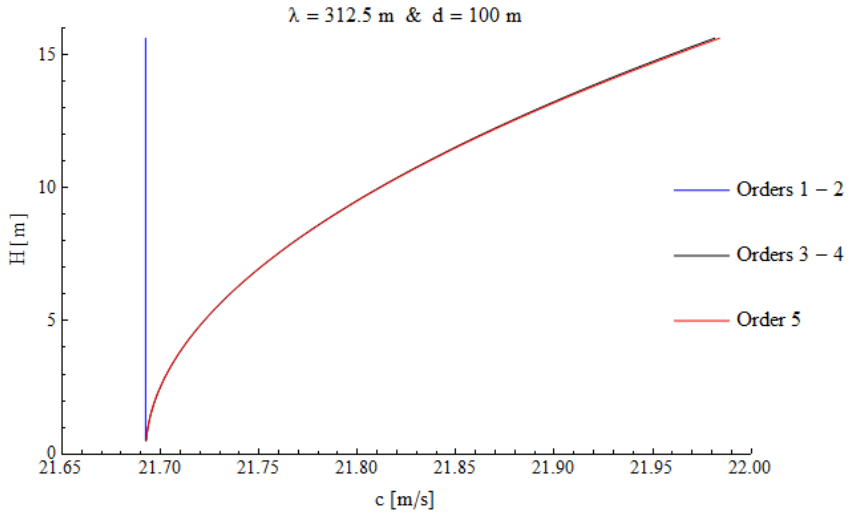

Figure 4.4: Variation of wave celerity along the wave height, for Stokes wave orders 1-5.

As we observe, for orders 1 and 2, the wave celerity is constant for all values of wave height. For orders 3-4 and 5, the variation is almost identical, since the two corresponding curves do not diverge.

Fenton gives the relations for the velocity potential Φ and the free surface elevation η as follows:

$$\Phi(x,z,t) = C_0(g/k^3)^{1/2}\sum_{i=1}^{5}\varepsilon^i\sum_{j=1}^{5}A_{ij}\cosh[j\,k(z+d)]\sin[j\,k(x-c\,t)] + \cdots \qquad (4.22)$$

$$\eta(x,t) = (1/k)\sum_{i=1}^{5}\varepsilon^{i}\sum_{j=1}^{5}B_{ij}\cosh[j\,k(x-c\,t)] + \cdots \qquad (4.23)$$

Here, the coefficients $A_{ij}$and B_{ij} are also given in table 3.1 and the parameters i and j are defined with respect to the order of the model, from one to five.

Then, in order to apply the Bernoulli's theorem for the construction of the mathematical problem, we need an expression for the constant R, which is also provided by Fenton,

$$R = (g/k)[\frac{1}{2}C_0 + \varepsilon^2 E_2 + \varepsilon^4 E_4 + \cdots] \qquad (4.24)$$

Finally, if we make use of the Bernoulli's equation, we can obtain the expression for the pressure p,

$$p(x,z,t) = \rho\,R - \rho\,g\,z - \frac{1}{2}[(u-c)^2 + w^2] \qquad (4.25)$$

The equations (4.21) to (4.24) formulate the mathematical model provided by Fenton for the description of the surface gravity waves motion with application of Stokes theory. Obviously, the first order model coincides with the problem described in the linear theory. It is fact, however, that most ocean waves are approached more satisfactorily with the fifth order problem.

Another issue that should be taken into account is that Stokes theory presents accurate results while the magnitudes of both $\varepsilon$and $\varepsilon/(kd)^3$are small [12]. This implies that the method should not be applied in the case of shallow water unless there is some modification to the term $\varepsilon/(kd)^3$. Last, the variation of the free surface as is given by Stokes theory is presented in figures 4.5 and 4.6, for a certain wavelength and water depth and for order one (linear wave) and five.

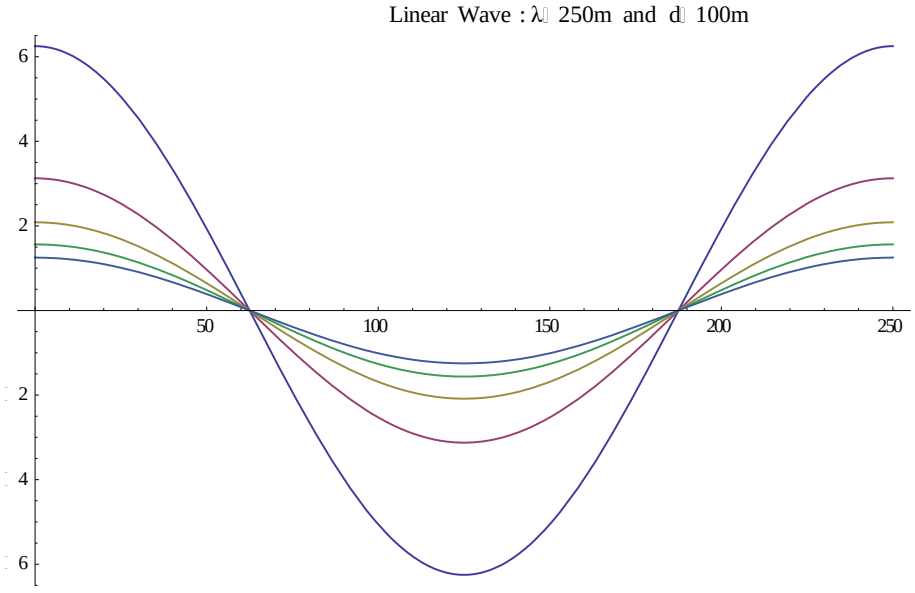

(a)

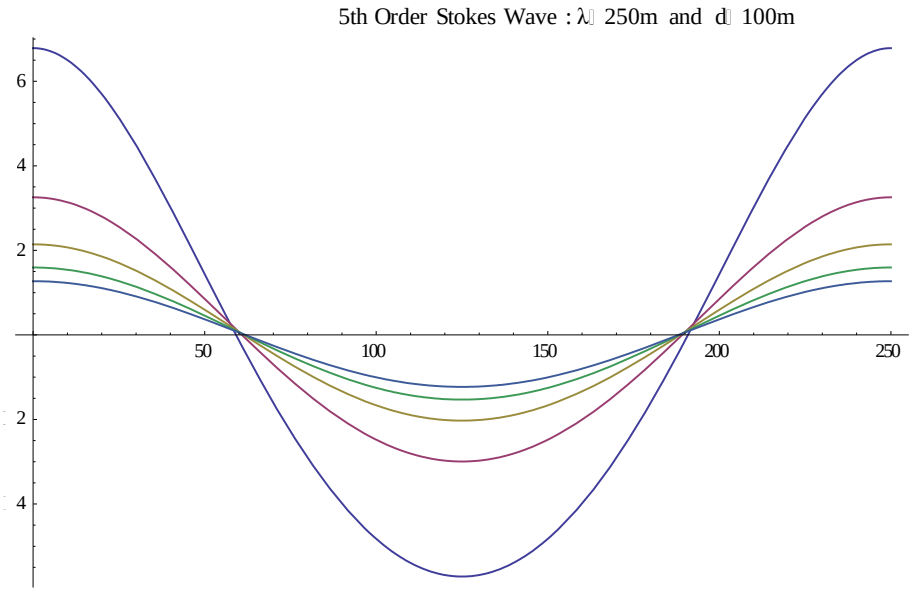

(b)

Figure 4.5: Alteration of the free surface elevation for different values of wave steepness (H/λ), for linear waves (a) and 5thOrder Stokes Wave (b).

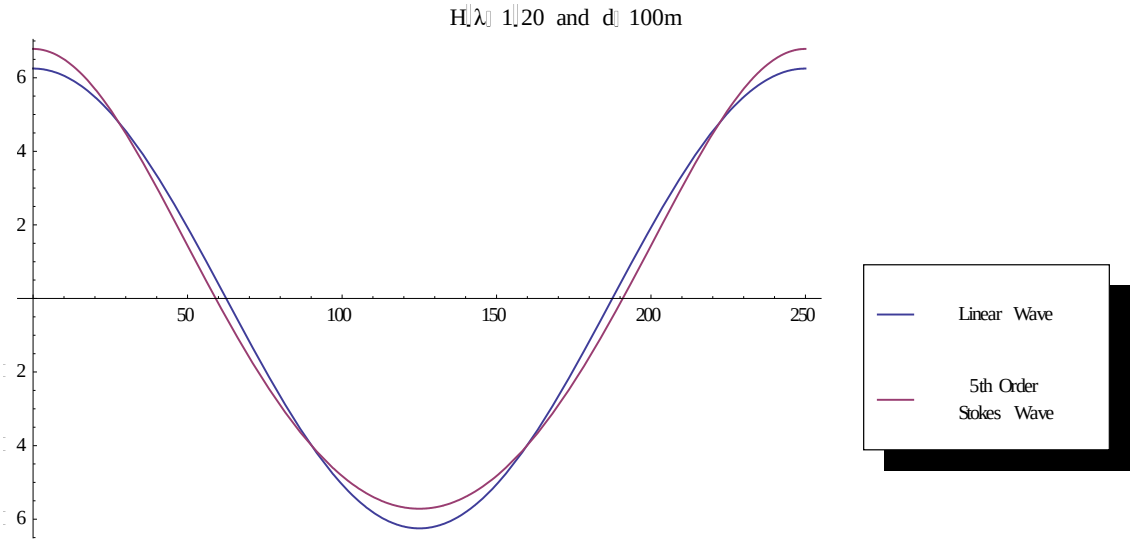

Figure 4.6: Alteration of the free surface elevation for Linear and 5th Order Stokes Wave.

5. ROLL STABILITY IN LONGITUDINAL WAVES

5.1 INTRODUCTION

In this chapter, we are going to examine two very important phenomena regarding the stability of a ship in longitudinal waves, such as parametric roll and pure loss of stability. At first, in chapter 5.2 we will analyze the physics of parametric roll resonance, i.e. the conditions on which the phenomenon can occur and the factors that have an influence on it. Then, in chapter 5.3 we will describe analytically how the stability changes while the ship is sailing in longitudinal waves, since this periodical variation constitutes the reason for the development of parametric roll resonance.

Subsequently, in chapter 5.4 we will construct the differential roll equation for a ship travelling in head or following seas, using the famous Mathieu equation at first and then inserting the factor of damping. Finally, in the last chapter 5.5 there is a short description of the phenomenon pure loss of stability, which is considered as one of the modes of stability failures in longitudinal waves.

5.2 PARAMETRIC ROLL RESONANCE

The phenomenon of parametric roll has been known to the naval architecture society for more than half a century [28]. A ship travelling in longitudinal seas experiences periodical variation of its transverse metacentric height i.e. its stability. Because of the hull geometry of a ship, especially as far as it concerns containerships with bow flare, stability increases when the ship is located in the wave trough, while it decreases when the ship is in the wave crest, as we will analyze later in chapter 5.3.

Parametric roll resonance occurs when the stability variation happens twice during one natural roll period, or else when the encounter frequency of the wave is nearly twice that of natural roll frequency [28]. This leads to the development of quite large roll angles (figure 5.1). However, roll equilibrium can be disturbed also in calm water, as a result of an external moment caused, for instance, by a wind gust or a transversal distribution of weight. In this case, the ship rolls with its natural roll frequency and the roll angles that are developed are similar to that in figure 5.1.

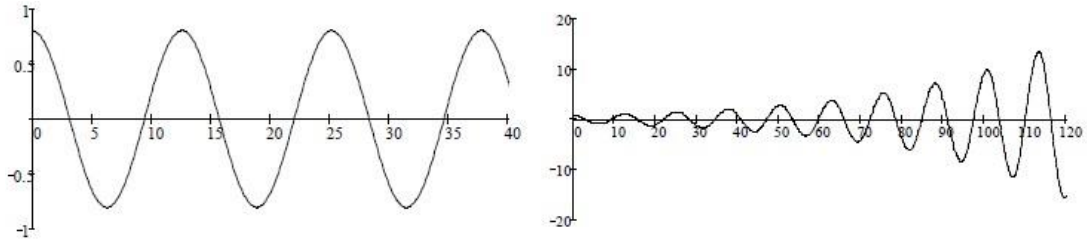

(α) (b)

Figure 5.1: Development of roll motions in calm water (a) and in parametric resonance (b) [28]

Parametric roll behavior intensifies when the encounter frequency of the waves is nearly twice the natural roll frequency, or when the stability is starting to increase. The latter condition states that the roll disturbance happens in the time interval between the wave crest, where the metacentric height is decreased, and the wave trough, where stability increases.

The development of parametric roll within time is shown in figure 5.2. At first, we observe that after a quarter of the period, roll angles start to become larger than they would have been in the absence of wave excitation moment, i.e. in calm water, and this difference is proportional to time. The figure 5.2 displays also the variation of the metacentric height within time, while the ship is sailing in longitudinal waves. The moment that the first quarter of the period has passed is the turning point where the value of GM becomes the initial one and the interia of the ship causes the latter to start rolling to the other side. After half a period, the ship is located in the wave crest, where stability decreases as we have already mentioned. Therefore, the roll angle is getting larger than the one corresponding to still water and the one that appears after the first quarter of the period. After one and a half period the ship is in the wave trough, where stability increases, and the value of roll angle is smaller than the one expected in calm water. The behavior described is repeated periodically, with the roll angles to continue to increase within time.

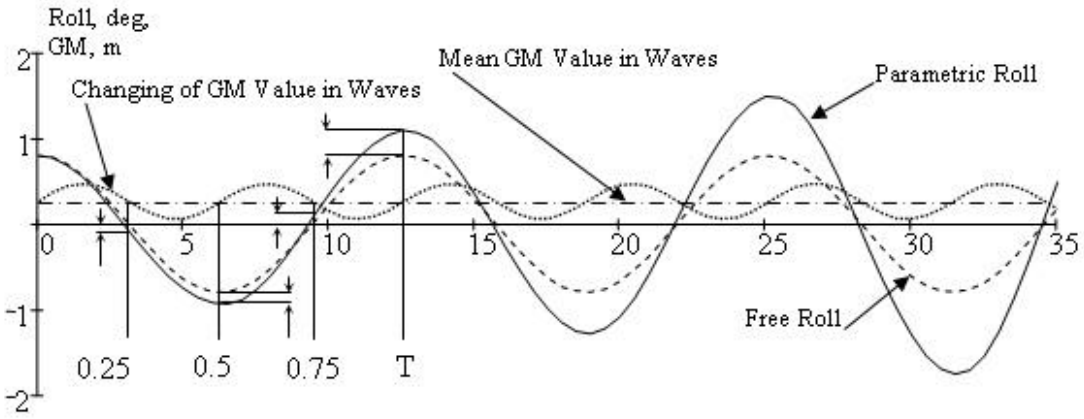

Figure 5.2 Development of parametric roll [28]

Another parameter that should be taken into account is the wave direction, i.e. whether the ship encounters following or head seas. Although the physical basis of parametric roll resonance is identical in both situations, in the case of head seas the ship is more likely to experience heave and pitch disturbance along with parametric roll and, therefore, the final motion of the ship becomes more complicated.

Whether parametric roll resonance will occur depends on the ratio of the natural roll frequency to the wave encounter frequency, $n=\omega_n / \omega$, as we have already discussed. Therefore, whether the phenomenon will take place in head or following waves depends mostly on two factors. One of them is the value of the initial GM in still water, since it relates to the natural roll frequency of the shipω_n. Another factor is the value of the wavelength,

which relates to the wave number *k* and the wave celerity *c*, on which the encounter frequency depends, for a certain value of ratio *n*.

5.3 CHANGE OF STABILITY IN WAVES

When a ship is exposed to an external heeling moment, stability is the measure of its ability to respond to that moment [2]. This response results as a component of hydrostatic and hydrodynamic pressures that apply to the submerged hull, since stability depends on the shape of the submerged portion of the hull. The distrortion of water surface along with the various motions of the ship (roll, heave, pitch) are responsible for the difference between the submerged hull geometry of a ship subjected to the action of waves and the static waterline. In this essay, only the hydrostatic nature of the response will be taken into account, as it is the most important one.

As it is given by the ship hydrostatics and stability theory, for small roll angles the metacentric height is given by the relation [35]:

$$GM = KB + BM - KG \tag{5.1}$$

With,

KB: the vertical distance of the center of buoyancy,

$\mathrm{BM} = \frac{\mathrm{I}}{\nabla}$, where

- I is the second moment of waterplane's area; and
- ∇ is the volume of displacement

KG: the vertical distance of centroid

The encounter frequency is quite low in following waves and we can assume that the ship is moving along the waves in a semi-balanced state around the vertical reference plane. Consequently, the volume of displacement *(∇)* is considered as constant.

The changes of the stability are intensified when the wave crest or the wave trough are amidships, for a wave with length comparable to the one of the ship's (figure 5.3). For most ships designed with bow flare, such as container ships, the waterline becomes more narrow forward toward the bow at the design waterline and wider at waterlines that are deeper.

When a ship with bow flare is located in the trough of a wave the stability is improved. That is because the waterline becomes wider in comparison to calm water, as relatively wide sections fore and aft are submerged. Consequently, the second moment of area of the waterplane *I* increases and so does BM. At the same time, KB seems to be slightly decreasing, as the submerged volume amidship is reduced. The increase of the BM is usually

greater than the decrease of KB and with KG,∇ being constant, GM increases too according to the relation 5.1.

However, when a wave crest is near amidships, the waterline becomes narrower as it intersects the thin parts of the hull sections fore and aft. Although KB may be increasing slightly due to the increment of the submerged hull volume in the midship section, the BM=I/∇ is getting lower. Therefore, stability decreases in this case.

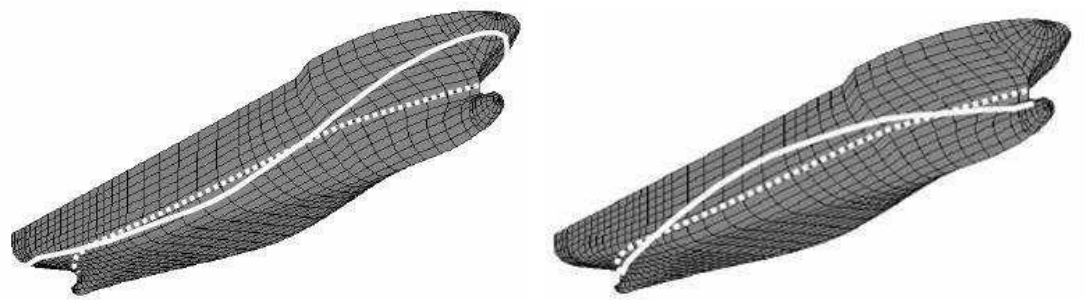

(a) *(b)*

Figure 5.3: Waterline in wave trough (a) and crest (b) in comparison to calm water. [2]

5.4 THE DIFFERENTIAL ROLL EQUATION

5.4.1 VARIATION OF METACENTRIC HEIGHT (GM)

In regular waves, the righting moment will present a sinusoidal variation with time between the extreme values [13]. Therefore, we can describe the one degree of freedom rolling motion of a ship in longitudinal (following or head) waves with a relation of motion close to that of still water. However, the restoring moment does not only depend on angle of heel, but is a sinusoidal function of time. For small roll amplitudes, we can assume that the metacentric height varies with time with an equation where the metacentric height is equal to the slope to the righting arm curve at the origin. The equation is as follows:

$$GM(t) = GM_o(1 + C\ cos\omega t) \tag{5.2}$$

Here,

GM_o: metacentric height in still water

C : fractional variation of GM due to waves, heave and pitch

ω : frequency of variation of GM or frequency of encounter of waves

5.4.2 THE MATHIEU EQUATION

For small amplitude roll motion, with absence of stimulation and damping, the equation of motion is given by

$$I_x \frac{d^2\varphi}{dt^2} + \Delta\, GM(t)\, \varphi = 0 \tag{5.3}$$

and if we introduce the relation of the GM variation (5.2) we obtain

$$I_x \frac{d^2\varphi}{dt^2} + \Delta\varphi(GM_o + CGM_o cos\omega t) = 0 \tag{5.4}$$

With,

φ: angle of roll,

Δ : ship displacement,

I_x: mass moment of interia in roll, including added mass effect

We need to define the natural roll frequency of the ship ω_n,

$$\omega_n{}^2 = \frac{\Delta GM_o}{I_x} \tag{5.5}$$

and the parameters δ, εas follows:

$$\delta = \frac{\Delta GM_o}{\omega^2 I_x} = \frac{\omega_n{}^2}{\omega^2}\,, \tag{5.6}$$

$$\varepsilon = \frac{C\Delta GM_o}{I_x\omega^2} = C\,\frac{\omega_n{}^2}{\omega^2}\,, \tag{5.7}$$

We divide now both sides by the mass moment of interia I_x. Therefore, the equation (5.4) becomes:

$$\ddot{\varphi} + \omega^2(\delta + \varepsilon\, cos\omega t)\varphi = 0 \tag{5.8}$$

The final equation (5.8) is known as the *Mathieu Equation* and is a linear differential equation with a time varying restoring coefficient. Even though it seems simple, there is no precise analytical solution to be given. Extensive studies of the various solutions have shown that the difficulty focuses on the unstable behavior of certain values of the frequency parameter, δ. The stability diagram for the Mathieu Equation is shown in figure 5.4, where the shaded areas represent the stable (δ, ε) pairs, for which roll motion cannot take place and the non-shaded regions are unstable, i.e. roll motion can exist.

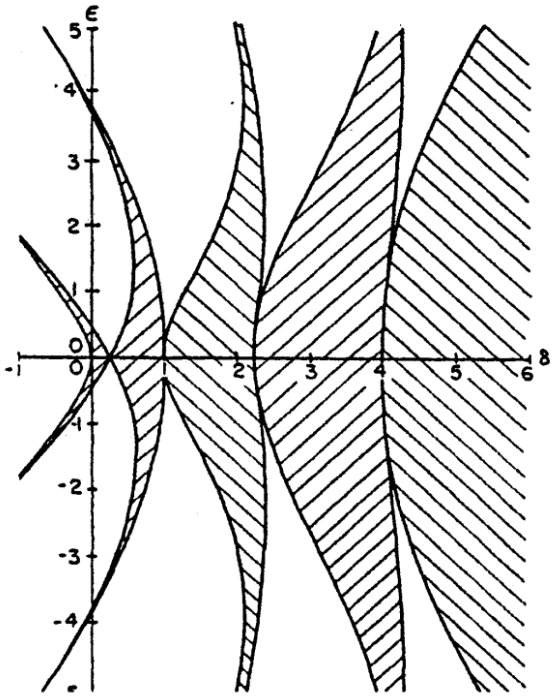

Figure 5.4: Stability Diagram for the Mathieu Equation [3]

If the pair (δ,ε) is located in an unstable region, a random initial disturbance will cause an oscillatory motion that will be increasing indefinitely with time. In a stable region, however, the initial disturbance will die out with time. From relations (5.6) and (5.7) we see that δ is the square of the ratio of the natural roll frequency of the ship to the wave encounter frequency, while εis proportional to the fractional variation of GM.

The characteristic of the Mathieu Equation is the fact that for $4\frac{{\omega_n}^2}{\omega^2} = n^2$, where n is whichever natural number, solutions corresponding to unstable regions can exist [2]. In case of$n = 1$, the natural roll frequency of the ship equals to the half of the wave encounter frequency ($\omega_n = {}^{\omega}/_{2}$) and then the phenomenon of *principal resonance* occurs. When $n = 1$ and $\omega_n = \omega$ we have *fundamental resonance*. There is no reason to investigate what happens for values of $n > 2$, because they do not apply to usual ships.

5.4.3 THE EFFECT OF DAMPING

Roll damping is a very significant factor in the development of parametric roll resonance. When a ship is sailing in calm water, oscillatory roll motion can occur by an impulsive disturbance in roll or roll velocity caused, for instance, by a wind gust. At this situation, the roll amplitudes decrease over consecutive periods due to the existence of roll damping [28], as shown in figure 5.5. The latter is a result of the waves and eddies that a rolling ship creates, along with the viscous drag that is exerted on the ship.

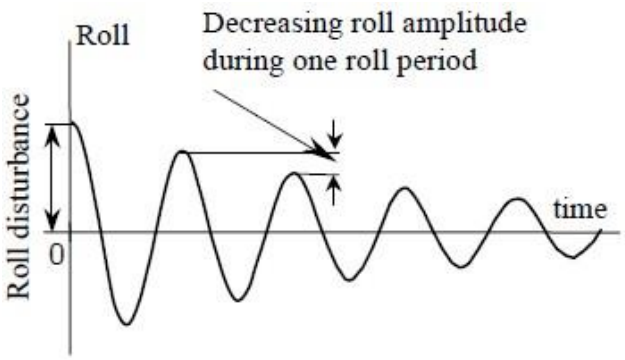

Figure 5.5: Consecutive decreasing roll amplitudes due to roll damping in calm water [28].

There is a damping threshold for parametric roll resonance. If the decrease of roll amplitude per period due to damping is greater than the increase of amplitude due to the change of stability in longitudinal waves, parametric roll resonance cannot develop since the roll angles will not increase. However, if the loss of amplitude is less than the gain, parametric resonance can occur.

If we introduce the effect of damping to the equation (5.3), we obtain the new differential roll equation

$$I_x\ddot{\varphi} + B\dot{\varphi} + \Delta\, GM(t)\, \varphi = 0 \tag{5.9}$$

where the alteration of GM is given by (5.2) and the (5.9) becomes

$$I_x\ddot{\varphi} + B\dot{\varphi} + \Delta\varphi(GM_o + CGM_o cos\omega t) = 0 \tag{5.10}$$

with B: the viscous roll damping coefficient

We divide again both sides of (4.8) by the mass moment interia I_x and we get

$$\ddot{\varphi} + +b_1\dot{\varphi} + \omega^2(\delta + \varepsilon\, cos\omega t)\varphi = 0 \tag{5.11}$$

where $b_1 = {}^{B_1}/_{I_x}$

Taking into account the effect of damping we expect the motion to be limited in amplitude. However, if the term of damping is linear, such as in (5.8), the only effect would be the rise of the threshold of value C for a certain frequency of variation, ω. Consequently, in order for the motion to be limited in amplitude, there must exist nonlinear damping similar to square or even higher power of the roll velocity [3].

5.5 PURE LOSS OF STABILITY

Along with parametric roll resonance, pure loss of stability is considered as one of the modes of stability failures in following seas [3]. Capsizing caused by pure loss of stability in

the wave crest in following waves was observed by Paulling during experiments in San Francisco Bay [3].

When a ship is sailing in following or stern quartering seas, the wave encounter frequency decreases. Therefore, the ship may spend a significant amount of time near the wave crest, which is the worst position for the stability of a ship as we have already discussed. As the restoring moment may be significantly decreased, the ship may suffer from large roll angles or even capsizing if it spends enough time in this unfavorable situation.

The critical factor for the phenomenon of pure loss of stability is the amount of time that the ship will spend in the situation of very low or even negative value of righting arm. Consideration of surging and surf-riding should also be taken into account for pure loss of stability [3]. In contrast to parametric resonance, where many wave lengths are needed in order for the vessel to capsize (if it eventually will), pure loss of stability can occur very quickly, after a period corresponding to only half of one wavelength.

6. METACENTRIC HEIGHT (GM) CALCULATION APPROACH

6.1 INTRODUCTION

In order to construct the stability charts for parametric roll resonance, we need to determine the variation of GM(t) as function of time. As known, GM results as a component of the vertical distance of the center of buoyancy (KB), the metacentric radius (BM) and the vertical distance of centroid (KG). The later depends only on the loading condition of the ship and therefore it remains constant while the ship is moving along with the waves. However, KB relates to the trim that applies on the ship in every position up on the wave, while BM (=I/∇) depends on the alteration of the watelplane area.

For the definition of the waterplane for each location of the ship, the local drafts of each station need to be calculated first. For every position of the ship there is certain value of trim and heave for which the equilibrium of forces and moments are satisfied. Consequently, the first stage of the process will be to construct the equilibrium equations whose solution will lead to the definition of the necessary values of heave and angle of trim, so that the local drafts can be calculated. Then, through linear interpolation we will find the corresponding local beams so that we can calculate the value of the second moment of area of the waterplane.

6.2 SAMPLE SHIP DATA

A large modern containership with the main particulars shown in Table 6.1 was chosen as a sample in this study.

Length overall	L_{oa}	250.000 m
Length between perpendiculars	L_{pp}	238.350 m
Breadth (moulded)	B	37.300 m
Depth to main deck (moulded)	D	19.600 m
Design draught (moulded)	T_d	11.500 m
Freeboard draught (moulded)	T_{frb}	12.500 m
Displacement at T_d = 11.500 m:	68014 t	
Displacement at T_{frb} = 12.500 m:	75729 t	

Table 6.1: Main particulars of the under study containership.

6.3 SECTIONAL AREA AND ITS CENTROID

The hull geometry of the ship being studied is described by forty seven theoretical sections. The sections are introduced in the MATHEMATICA environment as lists of points *(x,y,z)*. The first step of the sectional data processing is the construction of an interpolating function that for every value of draft between the boundaries *(z),* returns the corresponding value of semi-breadth *(y)*, for each station.

Subsequently, since we have obtained fully the geometry of all sections, we create functions that return respectively the value of the sectional area and its centroid, for a given station (i) as follows:

$$S(i,T) \text{ and } Z_c(i,T)$$

As we see, the sectional area and its centroid are functions of the local draft (T) at each station.

6.4 SHIP EQUILIBRIUM ON WAVE

According to the hydrostatics theory [9], the equilibrium of ship is achieved when the equilibrium of forces

$$B = \Delta \tag{6.1}$$

and the equilibrium of moments are satisfied

$$BX_B{}' = \Delta\, X_G{}' \tag{6.2}$$

Here,

B is the buoyant force

Δ is the ship's displacement and

$X_B{}'$, $X_G{}'$ are the ordinates of the center of buoyancy and the centroid of the ship, with respect to the system $O_bX_b'Z_b'$ shown in figure 6.1.

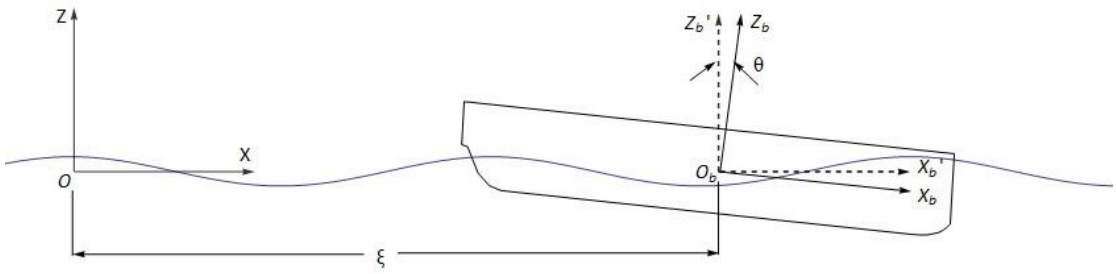

Figure 6.1: Coordinate system.

In the above figure 6.1 three coordinate systems are shown; OXZ, $O_bX_b'Z_b'$ and $O_bX_bZ_b$. The first one is moving along with the wave while the second is its parallel transfer in ξ. The

third system follows exactly the motion of the ship. Therefore, we need to make the following transformation

$$\begin{bmatrix} X_b{}' \\ Z_b{}' \end{bmatrix} = A \begin{bmatrix} X_b \\ Z_b \end{bmatrix} \tag{6.3}$$

where A is the rotation matrix and for the rotation angle θ of the system $O_bX_b{}'Z_b{}'$ to the system $O_bX_bZ_b$ (Figure 6.1), the expression (6.3) becomes

$$\begin{bmatrix} X_b{}' \\ Z_b{}' \end{bmatrix} = \begin{bmatrix} \cos(-\theta) & \sin(-\theta) \\ -\sin(-\theta) & \cos(-\theta) \end{bmatrix} \begin{bmatrix} X_b \\ Z_b \end{bmatrix} \tag{6.4}$$

Using the transformation above, we obtain the relations for the ordinates of the center of centroid

$$X_G{}' = LCG\ cos\theta - VCG\ \sin\theta \tag{6.5}$$

and the center of buoyancy

$$X_B{}' = LCB\ cos\theta - VCB\ \sin\theta \tag{6.6}$$

The longitudinal and vertical distance of the center of buoyancy that appear in the relation (6.6) are given by the hydrostatics theory [9] as

$$LCB = \frac{\iiint_{V_b} X_b\ dV}{V_b} \tag{6.7}$$

and

$$VCB = \frac{\iiint_{V_b} Z_b\ dV}{V_b} \tag{6.8}$$

where V_b is the volume of the submerged hull that can be written as

$$V_b = \iiint_{V_b} dX_b dY_b dZ_b = \int_{-L/2}^{L/2} dX_b \iint_{S_b} dY_b dZ_b = \int_{-L/2}^{L/2} S(X_b) dX_b \tag{6.9}$$

with $S(X_b)$ the sectional area corresponding to the local draft of the section, in the position X_b.

If we introduce the relation (6.9) to the expressions (6.7) and (6.8) we obtain

$$LCB = \int_{-L/2}^{L/2} X_b\ dX_b \iint_{S_b} dY_b dZ_b \left(\int_{-L/2}^{L/2} S(X_b) dX_b \right)^{-1} \rightarrow$$

$$LCB = \int_{-L/2}^{L/2} X_b S(X_b)\, dX_b \left(\int_{-L/2}^{L/2} S(X_b) dX_b \right)^{-1} \tag{6.10}$$

and

$$VCB = \int_{-L/2}^{L/2} Z_b\, dX_b \iint_{S_b} dY_b dZ_b \left(\int_{-L/2}^{L/2} S(X_b) dX_b \right)^{-1} \rightarrow$$

$$VCB = \int_{-L/2}^{L/2} Z_c(X_b)\, S(X_b) dX_b \left(\int_{-L/2}^{L/2} S(X_b) dX_b \right)^{-1} \tag{6.11}$$

where $Z_c(X_b)$ is the vertical coordinate of the centroid of the sectional area corresponding to the local draft of the section, in the positionX_b.

Using the relations (6.5), (6.6), (6.10) and (6.11), the equation for the equilibrium of moments (6.2) can be written now as follows:

$$cos\theta \int_{-L/2}^{L/2} X_b S(X_b)\, dX_b \left(\int_{-L/2}^{L/2} S(X_b) dX_b \right)^{-1} - sin\theta \int_{-L/2}^{L/2} Z_c(X_b) S(X_b)\, dX_b \left(\int_{-L/2}^{L/2} S(X_b) dX_b \right)^{-1} -$$

$$-LCG cos\theta + VCG \sin\theta = 0 \rightarrow$$

$$cos\theta \int_{-L/2}^{L/2} X_b\, dX_b - sin\theta \int_{-L/2}^{L/2} Z_c(X_b)\, dX_b - LCG cos\theta + VCG \sin\theta = 0 \tag{6.12}$$

The buoyant force is defined as $B = \rho\, g\, V_b$ and if we insert the relation for the V_b (6.9), the equation for the equilibrium of forces (6.1) becomes

$$\Delta = \rho\, g \int_{-L/2}^{L/2} S(X_b) dX_b \tag{6.13}$$

Finally, the equilibrium of the ship in every position on the wave is described by the system of equations (6.12) and (6.13).

6.5 SOLUTION OF THE EQUILIBRIUM EQUATIONS METHODOLOGY

The equations with respect to the equilibrium of the ship in each position on the wave that have been constructed in chapter 6.4 contain the terms of the sectional area and its

centroid. These terms depend directly on the values of local drafts in each section, as we have already mentioned in chapter 6.3. Therefore, we need first to calculate the local drafts in each section of the ship, for proceed to the solution of the system (6.12) and (6.13).

6.5.1 LOCAL DRAFT CALCULATION

The local draft of a section in the position X_s, where X_s is the distance between the section and the origin O_b is given by

$$T_S = T_o + Z_S + \tau \tag{6.14}$$

where,

T_o is the draft of the section in calm water [4]

Z_S is the free surface elevation with respect to the system $O_bX_bZ_b$

τ is the value of sinkage [5]

If the free surface elevation with respect to the system that is moving along with the wave OXZ is $\eta=\eta(x)$, the transformation into Z_S will take place as follows:

At first, we rewrite the relation (6.4) as

$$\begin{bmatrix} X_b \\ Z_b \end{bmatrix} = \begin{bmatrix} \cos\theta & \sin\theta \\ -\sin\theta & \cos\theta \end{bmatrix} \begin{bmatrix} X_b{}' \\ Z_b{}' \end{bmatrix} \tag{6.15}$$

and we obtain

$$X_s = Xcos\theta + \eta(\xi + X)sin\theta \tag{6.16}$$

and

$$Z_s = -Xsin\theta + \eta(\xi + X)cos\theta \tag{6.17}$$

where X is the root of the equation (6.16). We also remind that ξ is the distance between the two origins O and O_b.

6.5.2 BISECTION METHOD

The system of the equations (6.12) and (6.13) that compose the equilibrium of the ship on the wave will be solved numerically by making use of a code in the MATHEMATICA

[4] We have not taken into consideration the value of trim that the ship has in calm water, due to the load allocation, and therefore all section have the same local draft T_o in calm water.

[5] Where heave τ refers to either elevation or immersion and its value is positive for the last case (immersion).

environment. The latter has been created for the purpose of the current essay. The problem cannot be solved directly due to the mutual dependence of the equations on the values of angle of trim θ and heave τ. The latter may not be shown directly in the system (6.12) – (6.13), but enters in the calculation of the local draft in each section T_s *(eq. 6.14)* and consequently in the calculation of the sectional area and its centroid. The numeric code that has been created contains a bisection method routine that applies on both equations in a range of angles $\theta \in [\theta_a, \theta_b] = \left[-\frac{H\pi}{\lambda}, \frac{H\pi}{\lambda}\right]$and values of sinkage $\tau \in [\tau_\alpha, \tau_b] = [-\frac{H}{2}, \frac{H}{2}]$. In every step of the equilibrium of moments satisfaction, the equilibrium of forces must be always satisfied too. We note that the integrals that appear in the equations are calculated by the method of Simpson and the trapezoidal method. Finally, we obtain the unique pair $\{\theta_c, \tau_c\}$, for which the equilibrium of the ship is achieved in a specific position on the wave.

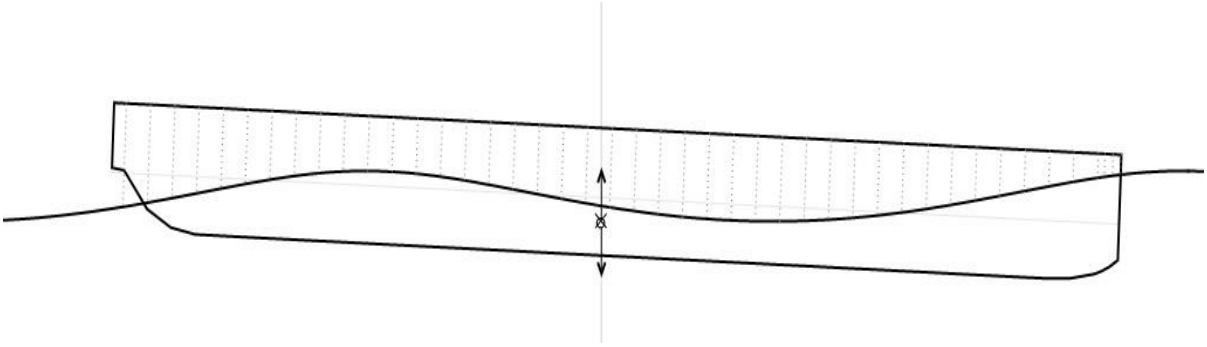

Figure 6.2 Equilibrium achieved at position x, for $\{\theta_c, \tau_c\}$.

At this point, we need also to note that after the process of the bisection method, the final position of the ship on the wave x_f will be slightly different from the original position x_o ,since the latter needs to be transformed as

$$x_f = x_o + \tau_c \cdot \sin\theta_c \tag{6.18}$$

6.6 CALCULATION OF METACENTRIC HEIGHT (GM)

At a random position of the ship on the wave *x*, the value of the metacentric height is given, as known, by

$$GM_x = VCB_x + \frac{I_{T_x}}{V_b} - VCG \tag{6.19}$$

Here,

VCB_x is the vertical distance of the center of buoyancy at the position x on the wave, after the equilibrium of forces and moments have been satisfied, as calculated by the code constructed in the MATHEMATICA environment.

I_{T_x} is the second moment of area of the waterplane at the specific position *x* on the wave. Generally, the latter is given by the hydrostatics and stability theory [9] as follows

$$I_T = \frac{2}{3} \int_{-L/2}^{L/2} {b_{X_s}}^3 \, dX_b \tag{6.20}$$

Here, b_{X_s} is the local beam of the section in the position $X_s$with respect to the local draft T_s. The latter is calculated as described in chapter 6.5.1, while the local beams are obtained through linear interpolation of the local drafts, as already mentioned. In addition, the second moment of area of the waterplane is calculated by making use of the method of Simpson.

Last, the submerged volume of the hull V_b , as long as the vertical distance of the centroid VCG, remain constant while the ship is moving along with the wave. They depend only on the loading case of the ship that is chosen for the calculations. Finally, we calculate the value of the metacentric height by making use of the expressions (6.19) and (6.20), for quite enough positions up on the wave, from one wave trough to another, and we obtain pairs of (x, GM_x)that describe fully the alteration of the stability while the ship is sailing along with the wave. The following figures represent the variation of the metacentric height in one wave length, for various values of wave steepness.

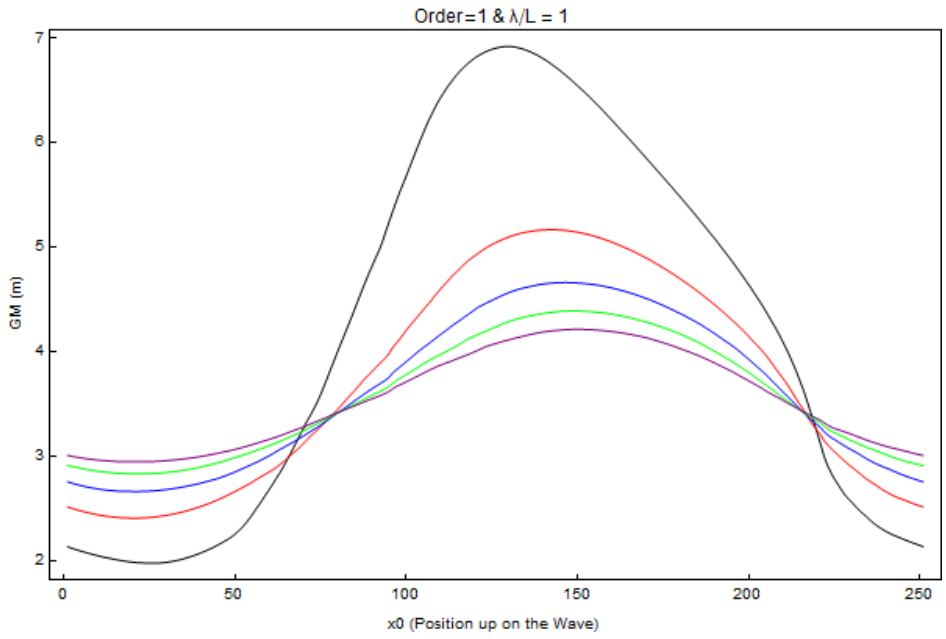

Figure 6.3: Metacentric height curve as a function of the position of the ship up on the wave x, for various values of wave steepness, λ/L=1 and for linear wave (Order=1).

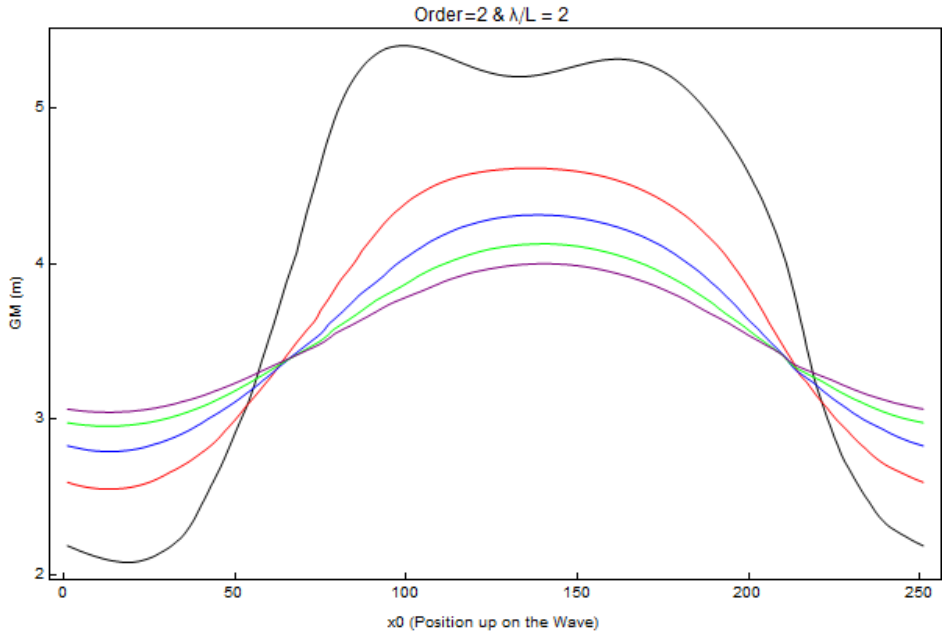

Figure 6.4: Metacentric height curve as a function of the position of the ship up on the wave x, for various values of wave steepness, λ/L=2 and for Order=2.

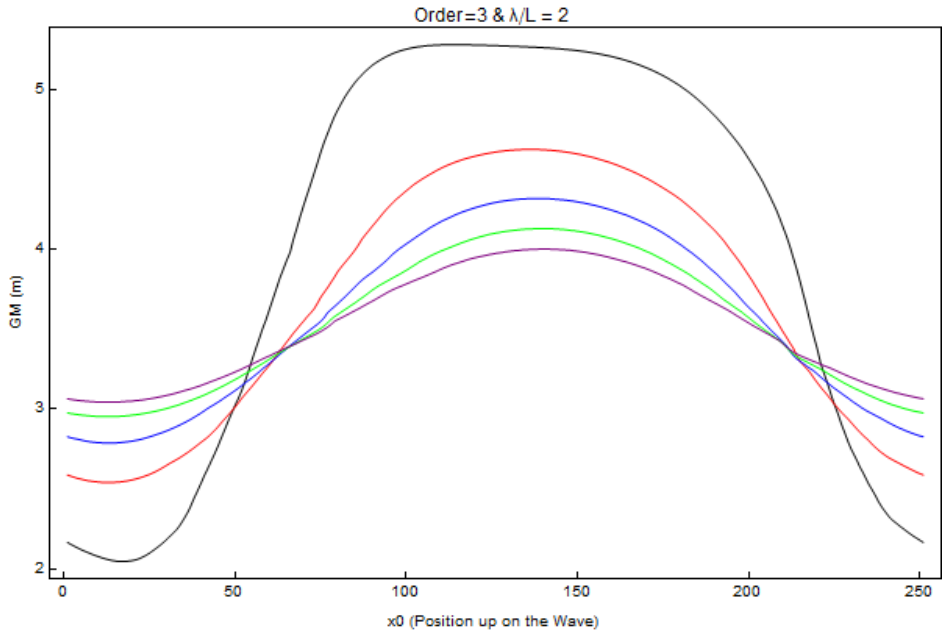

Figure 6.5: Metacentric height curve as a function of the position of the ship up on the wave x, for various values of wave steepness, λ/L=2 and for Order=3.

6.7 VALIDATION

6.7.1 PART I: COMPARISON TO LOADING MANUAL

It is important to ensure that the results obtained from the code in MATHEMATICA are valid. The first step will be to compare the value of the initial metacentric height GM_o in still water as received from our code, to the one given by the loading manual of the ship, for a certain loading case. For the selected loading condition, our numeric code gives us the following value of metacentric height

$$GM_o{}^{code} = 2.786\, m$$

The real value of GM_o as received from the loading manual of the under study containership is

$$GM_o{}^{real} = 2.848\, m$$

and the difference between the two values is

$$\frac{(GM_o{}^{real} - GM_o{}^{code})}{GM_o{}^{real}} 100\% = 2.19\%$$

The difference above owes its existence mainly to the fact that the geometrical approach of the ship does not contain elements such as bilge keels or the propeller. In addition, there is lack of information as long as it concerns the hopper and the bulb of the ship. Nevertheless, the difference between the two values is quite small and therefore we presume that our code gives quite satisfactory results for the case of still water. We need now to examine what happens when the ship is located in a position on a wave with given characteristics.

6.7.2 PART II: COMPARISON TO MAXSURF

The second step will be to compare the variation of GM along with the wave as obtained by our numeric code, with the one received from the designing program MAXSURF. At first, we introduce the sectional data of the ship into the environment of MAXSURF/Modeler. The hull geometry that is obtained is shown in figure 6.6.

Subsequently, we introduce the model into the environment of MAXSURF/Stability. There, we create a sinusoidal wave and we apply the equilibrium of the ship on the wave, from one wave crest to another. After the equilibrium of the ship has been achieved for the random position x on the wave, we receive the value of metacentric height that corresponds to that position. This process repeated for twenty times, i.e. we get twenty pairs of(x, GM_x).

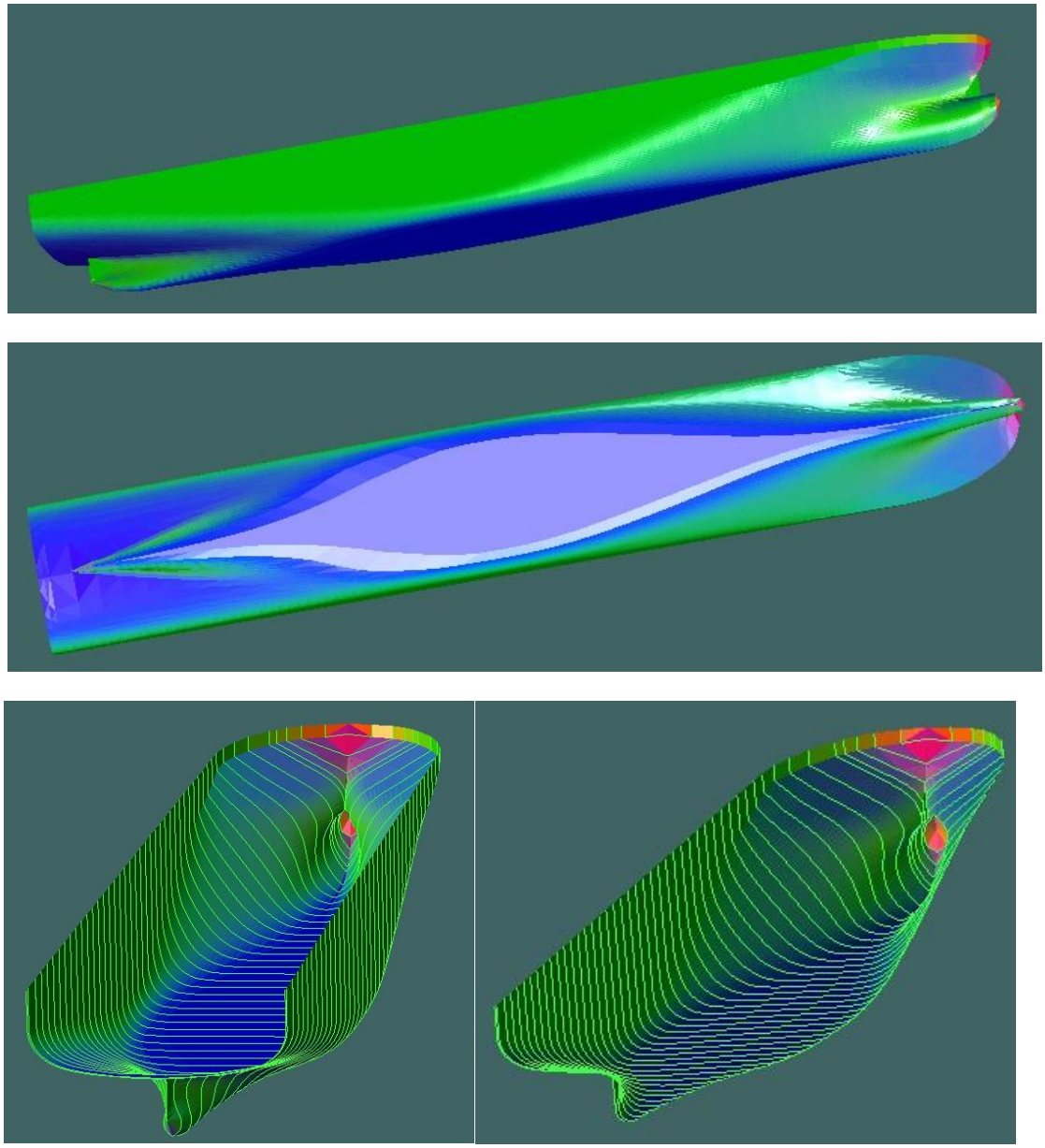

Figure 6.6: Hull geometry of the ship after its introduction into the environment of MAXSURF/Modeler.

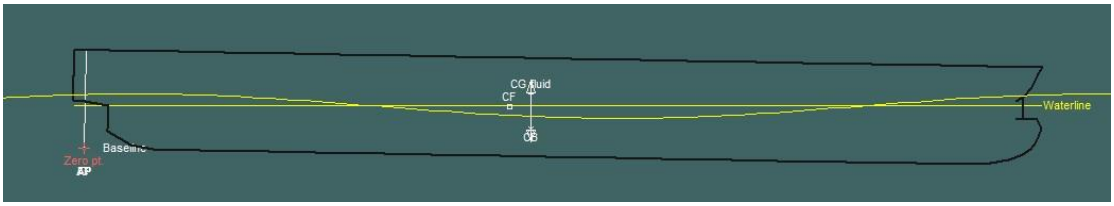

Figure 6.7: Equilibrium of the ship at the random position x on the wave, as calculated by MAXSURF/Stability.

In the following figure 6.8, the waterplane area of the ship is shown, while the ship is located, respectively, at the wave crest (upper figure) and at the wave trough (lower). As expected, the area of the waterplane is wider in the second case and the stability of the ship is increased.

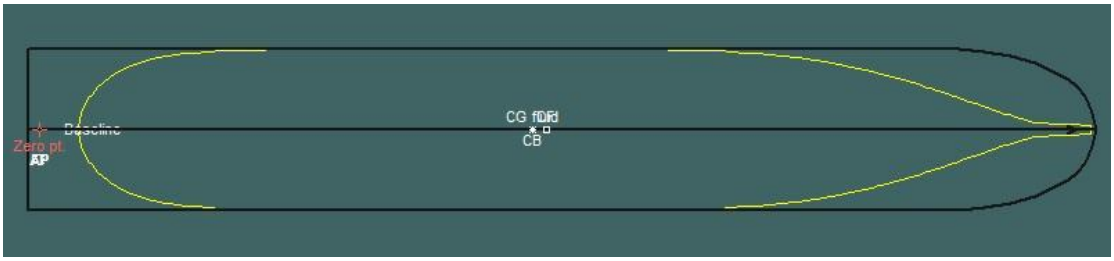

(i)

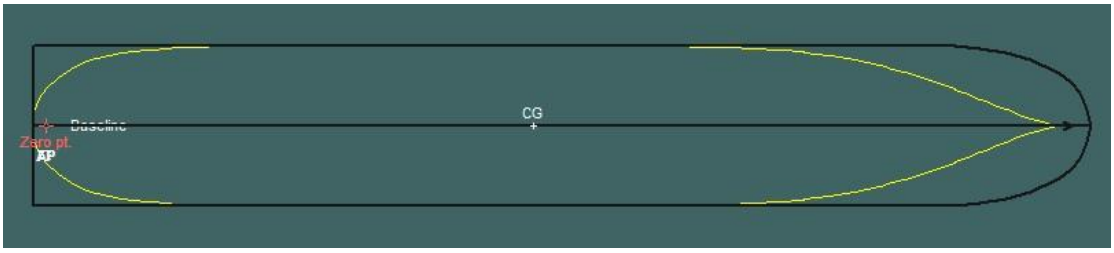

(ii)

Figure 6.8: Alteration of the waterplane area while the ship amidships is at the wave crest (i) and at the wave trough (ii), from MAXSURF/Stability.

Next, for the same wave characteristics and for Stokes wave order equal to one (the sinusoidal wave), we obtain twenty pairs of $(x, GM_x)$by making use of our numeric code in MATHEMATICA. Finally, we create the curves of GM as a function of x that correspond to MATHEMATICA and MAXSURF results, for three different wave characteristics, as shown in the following figures.

In these figures we observe that the two curves of (x, GM_x) are quite close, especially in the first case (i), where they are almost identical. It seems that the methodology on which the numeric code is based is similar to the one used in MAXSURF. The small divergences that occur can be explained by the different approach of the hull geometry between the two methods. The code in MATHEMATICA applies on the sectional data the method of Simpson for the approximation of the hull, while MAXSURF/Modeler uses NURBS surfaces for the construction of the full form [39].

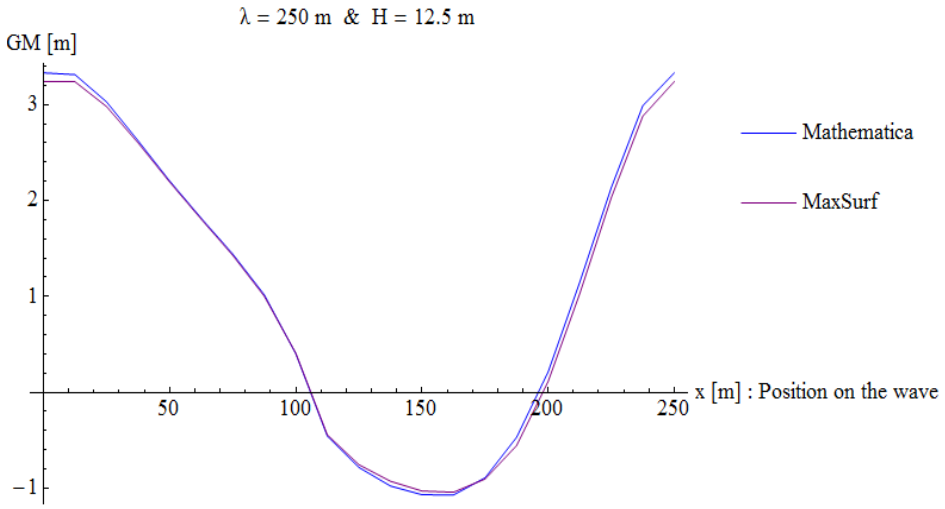

(i)

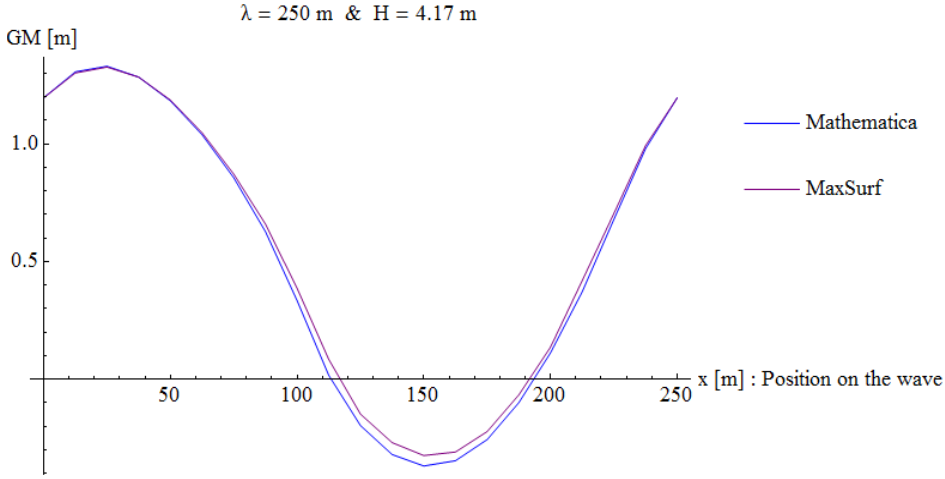

(ii)

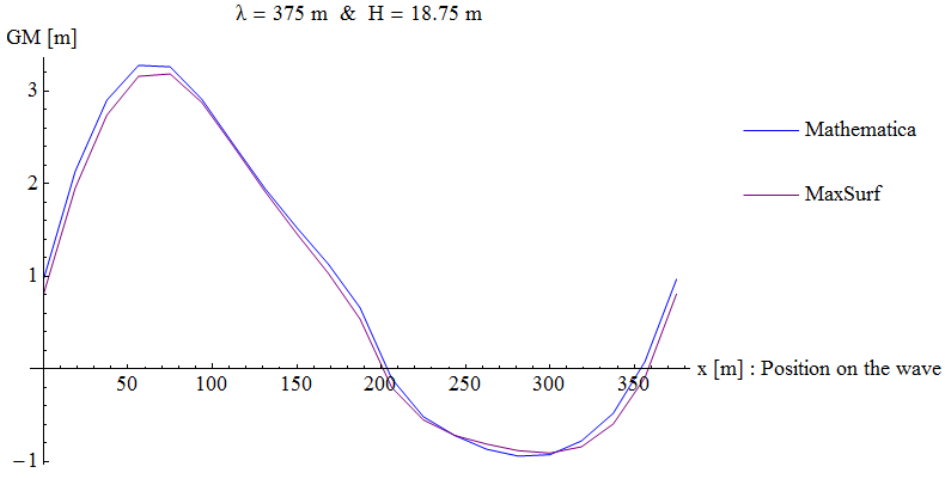

(iii)

Figure 6.9: Metacentric height alteration for one wavelength, as obtained from MATHEMATICA, in comparison to MAXSURF results, for three different wave characteristics.

7. METHODOLOGY OF STABILITY CHART CONSTRUCTION FOR PARAMETRIC ROLL RESONANCE

7.1 INTRODUCTION

In the current chapter we will develop the methodology on which the construction of the stability chart for parametric roll resonance is based. The horizontal axis of the chart will be the term α, which is analogous to the ratio of the wave encounter frequency ω_e to the natural rolling frequency of the studied containership ω_o,

$$\alpha = 4\frac{{\omega_o}^2}{{\omega_e}^2} \tag{7.1}$$

The vertical axis will be the ratio of the wave height to the wavelength, or else the wave steepness H/λ.Therefore, we are going to solve the differential roll equation for all values of $\alpha$and H/λ. The model of the equation is presented analytically in chapter 7.3. As known from the theory of parametric roll, parametric resonance occurs when the angles of roll start to increase within time. Consequently, if the solution of the differential equation gives a successive increment of the roll angle and if the latter surpasses a threshold value, we will consider that parametric roll resonance will occur for the pair $(\alpha, H/\lambda)$.

The range of $\alpha$is based on which region of instability we wish to study. In chapter 4 we noted that the ship is more likely to experience parametric roll resonance when the term α is nearly equal to one, i.e. when the natural rolling frequency of the ship is nearly half of that of the wave encounter. For the calculation of the natural rolling frequency ω_o of the ship, we are going to make use of an approximating expression provided by IMO. As far as it concerns the wave encounter frequency, it is defined automatically by the favorable range of a, as occurs from the relation above (7.1). In addition, there is a linear dependence of the wave encounter frequency to the wave celerity and the speed of the ship, as we will see in chapter 7.5.

7.2 REFERENCE SYSTEM

We assume that the reference system that follows the motion of the ship is moving along with the wave, as shown in figure 7.1.

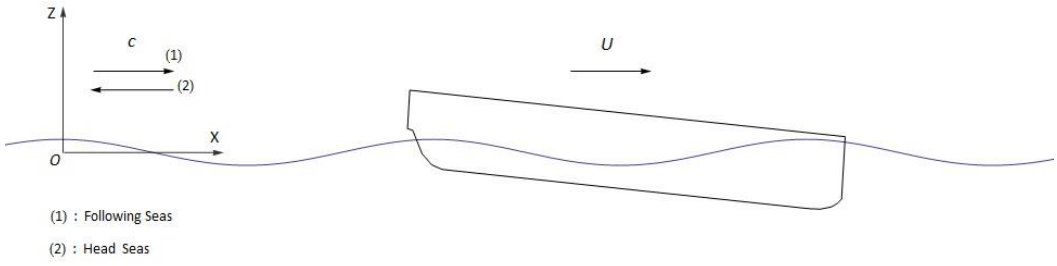

Figure 7.1: Reference system.

Therefore, the speed of the ship as followed by the reference system is

$$V = U - c \tag{7.2}$$

Where,

U is the constant speed of the ship; and,

c is the wave celerity

7.3 LINEAR DIFFERENTIAL ROLL EQUATION WITH DAMPING

The differential roll equation with damping that is introduced in chapter 5.4.3 can be rewritten as follows

$$\ddot{\varphi} + b_1\dot{\varphi} + \frac{\Delta\, g}{I_x}\, GM(t)\, \varphi = 0 \tag{7.3}$$

Here, $b_1 = B_1/I_x$, with B_1 the viscous damping coefficient as given by Spyrou [2], which is presented in the following relation

$$B_1 = \frac{2\,\zeta}{\sqrt{\Delta\, g\, I_x GM_o}} \tag{7.4}$$

The coefficient ζ is usually about 0.05 and for usual ships it does not become greater than 0.2 [2].

Subsequently, we consider the following initial conditions

$$\varphi(t = 0) = 0\, rad \tag{7.5}$$

and

$$\dot{\varphi}(t = 0) = \frac{\pi}{180}\frac{rad}{s} \tag{7.6}$$

In equation (7.1) we see that the variation of GM is within time, whereas the methodology of the GM calculation presented in chapter 6 provides a variation of GM along the wavelength, i.e. pairs of (x, GM_x) , where x is the position of the ship on the wave, and not a function of time. Since we assume that the ship is travelling with constant speed *U*, we easily overcome this obstacle by making the following transformation

$$x = x_o + V\, t \tag{7.7}$$

Where,

x is the position of the ship on the wave

x_o is initial position of the ship up on the wave (wave crest or wave trough)

t is the amount of time that the ship encounters a range of waves

V is the velocity of the reference system described in chapter 7.2.

Therefore, we introduce the variation of GM as pairs of (x, GM_x) into the equation (7.3), where x is now a function of time. The amount of time that we will consider for the solution of the differential roll equation will be with respect to the given wave encounter frequency, as follows

$$t \in \left[0\,, cycles \cdot \left(\frac{2\pi}{\omega_e}\right)\right]$$

Here, $cycles$ is the number of waves that we assume the ship will encounter during its travel. The variation of GM, however, has been calculated for one only wavelength, from one wave trough to another. Nevertheless, since the waves that we examine are periodical and do not alter their characteristics within time, we can presume that GM variation is also constant for every $cycle$ $[0\,, 2\pi]$.

7.4 NATURAL ROLLING PERIOD APPROACH

The natural rolling frequency of the ship is given by the relation in chapter 5.4.2 and can be written as

$$\omega_o = \sqrt{\frac{\Delta\ g\ GM_o}{I_x}} \tag{7.8}$$

Here, GM_o is the initial metacentric height of the ship for a given loading condition, provided by the loading manual of the ship studied.

Since we do not have any information for the mass moment of interia (plus added mass) I_x, we cannot calculate the natural rolling frequency directly through the expression (7.8). The International Maritime Organization (IMO) provides an approximate method for the calculation of natural rolling period in his paper MSC/Circ.707 [40], as a function of the ship's main particulars and the metacentric height in still water

$$T_R = \frac{2\ C\ B}{\sqrt{GM_o}} \tag{7.9}$$

With,

$$C = 0.373 + 0.023\frac{B}{d} - 0.043\frac{L}{100} \tag{7.10}$$

Here, B, d and L are respectively the breadth, the draught of the ship hull and the length between perpendiculars of the ship.

Therefore, the natural rolling period, as provided by IMO, changes only when the considered loading case of the ship alters, since the latter is connected directly to both the

initial metacentric height and the draught. Finally, we can calculate the natural rolling frequency as

$$\omega_o = \frac{2\pi}{T_R} \tag{7.11}$$

and if we introduce into (6.10) the expression (6.8) we obtain

$$\omega_o = \frac{2\pi\sqrt{GM_o}}{2\ C\ B} \tag{7.12}$$

Last, the mass moment of interia including the added mass effect I_x is given by the relation (7.8) as

$$I_x = \frac{\Delta\ g\ GM_o}{{\omega_o}^2} \tag{7.13}$$

7.5 WAVE ENCOUNTER FREQUENCY

The wave encounter frequency depends on three factors; the speed of the ship, the wave celerity and whether the encounter waves are following or head seas. It is obvious that in the case of head seas the wave encounter frequency increases significantly, whereas in the case of following seas it is the period of encounter between the waves and the ship that becomes greater. The wave encounter frequency is defined from Lloyd [41] as follows.

$$\omega_e = \frac{2\pi}{\lambda}(c - Ucos\mu) \tag{7.14}$$

Here,

c is the wave celerity

U is the constant speed of the ship

μ is the heading angle

The heading angle is defined as the angle as the angle between the direction of the ship and the direction of the wave. Therefore, as long as it concerns longitudinal waves along with the ship, the angle μtakes the following values

- $\mu = 0^o$: for following waves, i.e. the waves and the ship travel in the same direction
- $\mu = 180^o$: for head waves, i.e. the waves and the ship travel in the opposite direction

Consequently, the relation (7.14) can be rewritten as follows

$$\omega_e = k\ (c \pm U) \tag{7.15}$$

Where, $(+)$corresponds to the case of head seas, since the encounter frequency must increase, and $(-)$ corresponds to the case of following seas.

The desirable range of the axis αin the stability chart that will be created defines also the range of the wave encounter frequency, since the natural rolling frequency remains constant, for a specific loading case. If we assume that the waves that encounter the ship are following seas, the speed of the ship is given by

$$U = c - \frac{k}{\omega_e} \tag{7.16}$$

If the value of U is positive, then the assumption of following waves is right. On the contrary, if the relation (7.15) gives a negative value of U, we conclude that the waves that encounter the ship with the given frequency ω_e are head seas. At this point, it is worth to highlight that the combination of the relations (7.2) and (7.16) show that the velocity *V* of the reference system that is included indirectly in the differential roll equation, is actually nondependent to the wave celerity *c*.

7.6 STABILITY CHART CONSTRUCTION

The stability chart for parametric roll resonance corresponds to a specific wavelength λ and as long as it concerns its construction, we need to examine the ship's resonance in a range of $\alpha = 4\frac{{\omega_o}^2}{{\omega_e}^2}$ and wave steepness $\frac{H}{\lambda}$. In order to find the pairs of $\left(\alpha, \frac{H}{\lambda}\right)$ for which parametric roll resonance occurs after a given period of time, we created a numeric code in the environment of MATHEMATICA that solves repeatedly the linear differential roll equation described in chapter 7.3, for all values of α and $\frac{H}{\lambda}$.

The variation of the metacentric height required for the solution of the rolling equation is provided by the other numeric code in MATHEMATICA, the methodology on which the latter is based has been presented in chapter 5. We obtain pairs of (x, GM_x) for twelve different values of wave steepness, but for the same wavelength. Then, we create an interpolating surface of the metacentric height variations, so that we can obtain the variation of GM along the wavelength, i.e. the pairs of (x, GM_x), for whichever value of wave steepness between the boundaries, as shown in figure 7.2.

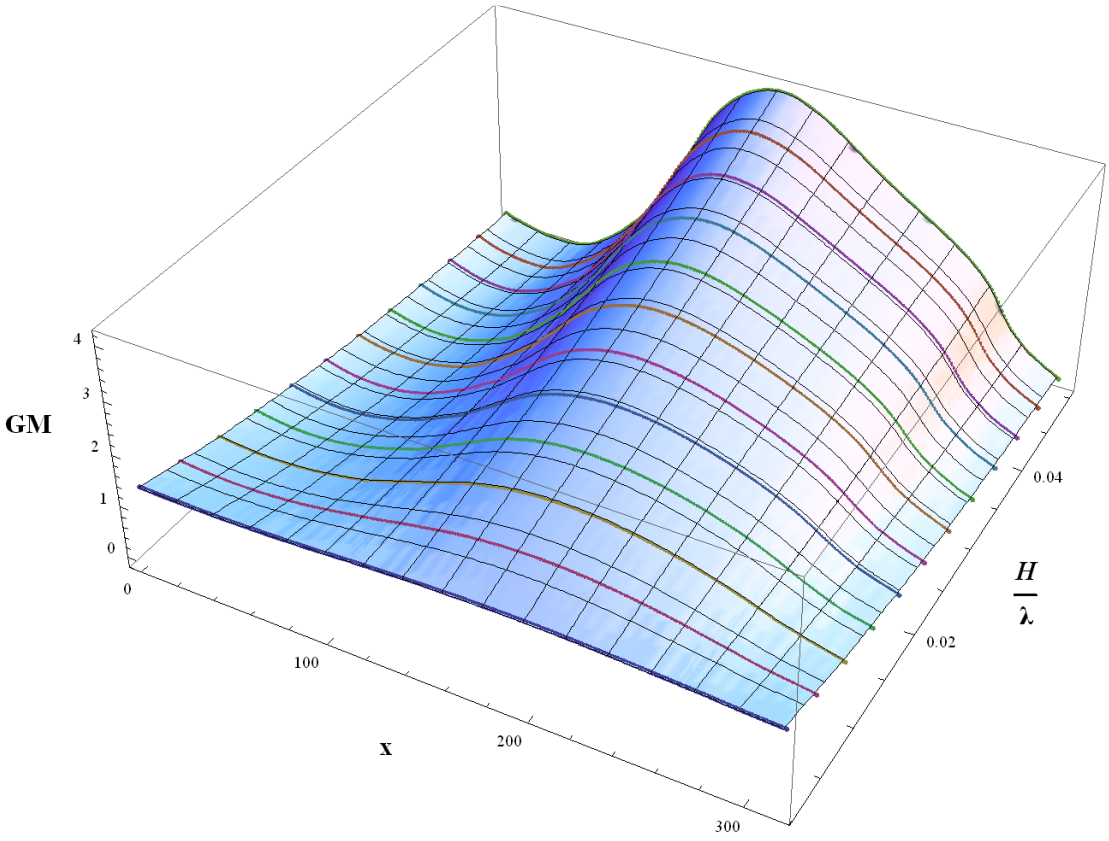

Figure 7.2: Interpolating Surface of GM variations, where the longitudinal axis corresponds to the position of the ship on the wave (x), the transverse axis corresponds to the value of wave steepness $\left(\frac{H}{\lambda}\right)$ *and the vertical axis corresponds to the value of metacentric height (GM).*

Solution of the differential roll equation will give the alteration of the roll angle φ with time, for every pair of $\left(\alpha, \frac{H}{\lambda}\right)$. The roll angles are expected either to increase or to decrease successively with time, as shown in figure 7.3.

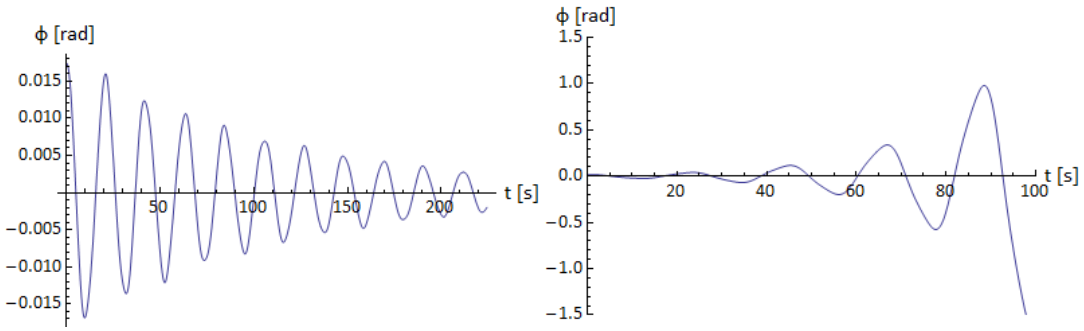

Figure 7.3: Variation of roll angles with time.

In the second case, where the roll angles increase with time, if they reach a given value of threshold within a given number of cycles, parametric roll resonance will occur and the corresponding pair of $\left(\alpha, \frac{H}{\lambda}\right)$ will be marked as unstable (Figure 7.4).

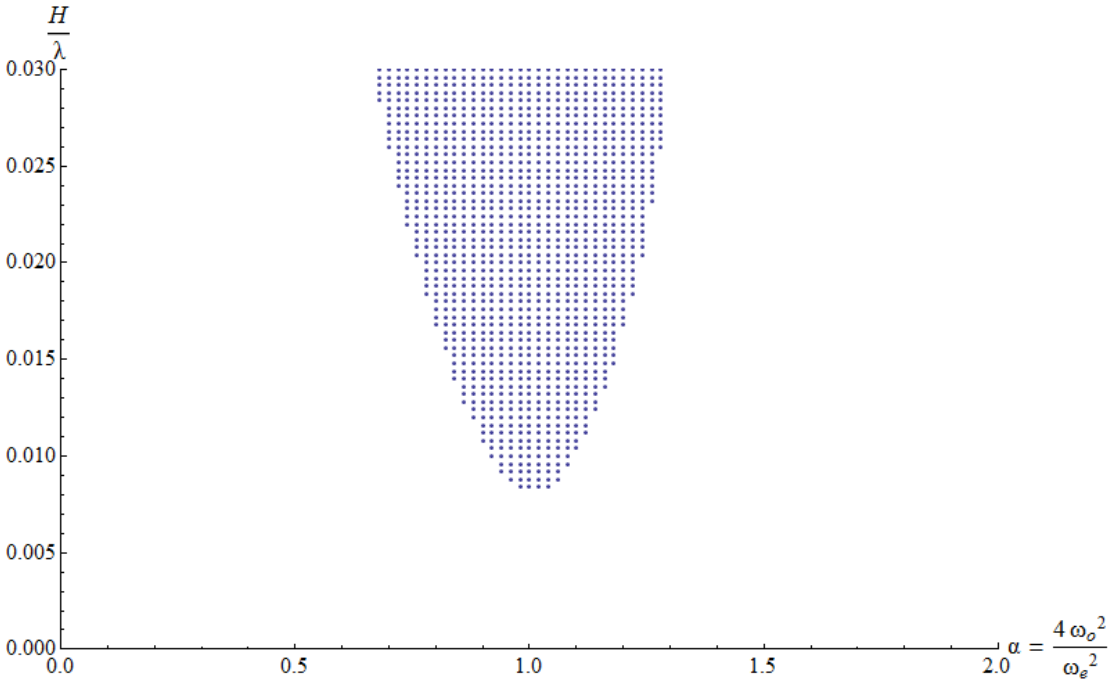

Figure 7.4: Example of stability chart for parametric roll resonance.

8. APPLICATIONS

8.1. SELECTED LOADING CASES

Four different loading cases were chosen from the loading manual of the containership, all in Full Load Departure (FLD), two in the scantling draft and two in the design, as shown in table 8.1.

Loading Case (LC)	Homogenous Weight γ_{hom} [t/TEU]	Draft [m]	Initial Metacentric Height: GM_o [m]	Vertical Distance of Centroid (Fluid) KG_{fl} [m]
15	12	12.517 (Scantl.)	0.494	17.17
18	16	12.517 (Scantl.)	1.480	16.21
30	12	11.519 (Des.)	2.052	15.62
36	16	11.519 (Des.)	2.848	14.83

Table 8.1 : Characteristics of the chosen loading cases.

The loading cases were selected in such way that the whole range of drafts and initial metacentric heights is covered.

8.2. VARIATIONS OF METACENTRIC HEIGHT (GM)

For the final purpose of construction of stability charts later, the variation of metacentric height along the wave is required first. Therefore, the methodology described in chapter 6 is applied on all loading cases, for all wave orders from one to five and for the same range of wave steepness. It also noted that all calculations are made for one value of wavelength:

$$\lambda = 1.5L_{oa} = 312.5m$$

The range of wave steepness is,

$$\frac{H}{\lambda} = 0.0015 \div 0.05$$

Therefore,

$$H = 0.47 \div 15.6\,[m]$$

Some indicative variations of the metacentric height are presented in the current chapter. The curves that are created are compared in two foci: between the values of wave steepness and between the wave order.

8.2.1. COMPARISON BY WAVE STEEPNESS

In the following figure 8.1, GM curves as functions of the position of the ship on the wave are shown. Each indicative diagram corresponds to one of the four considered loading conditions and to one wave order, from one to five.

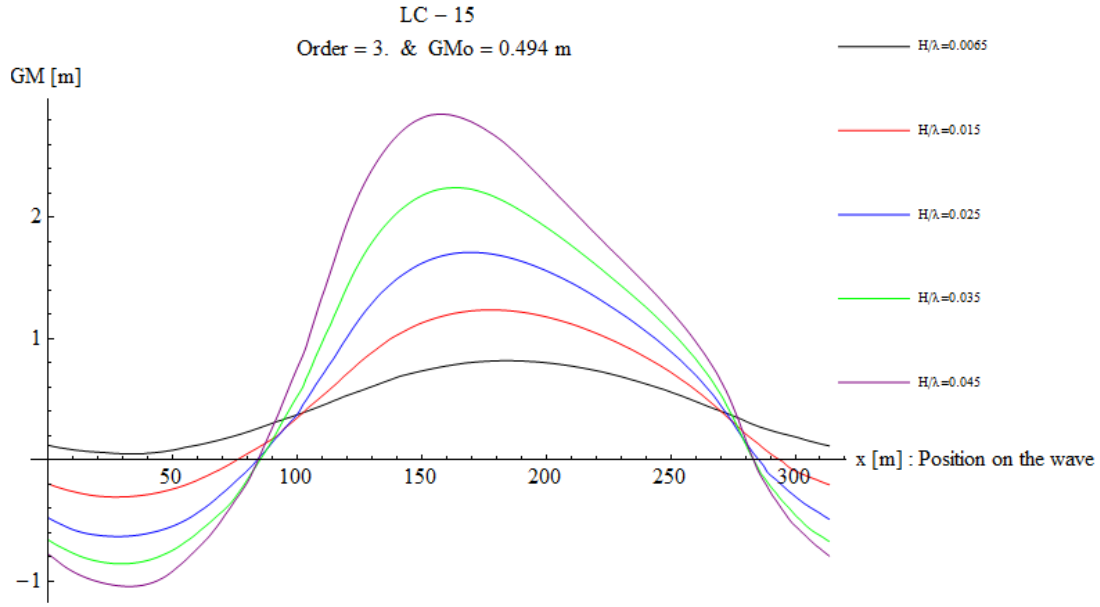

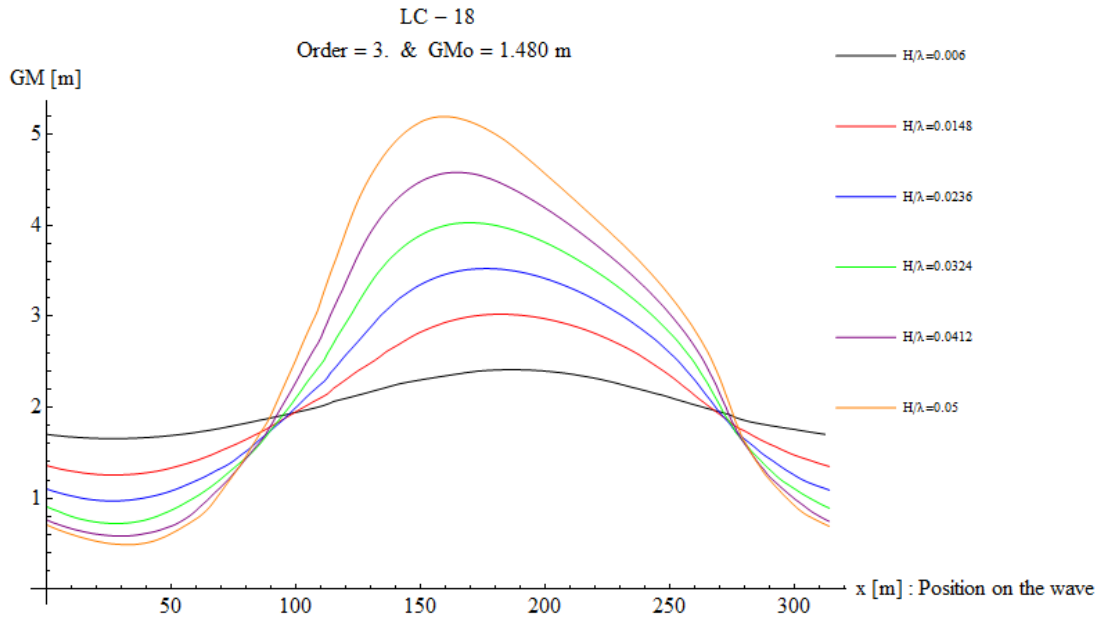

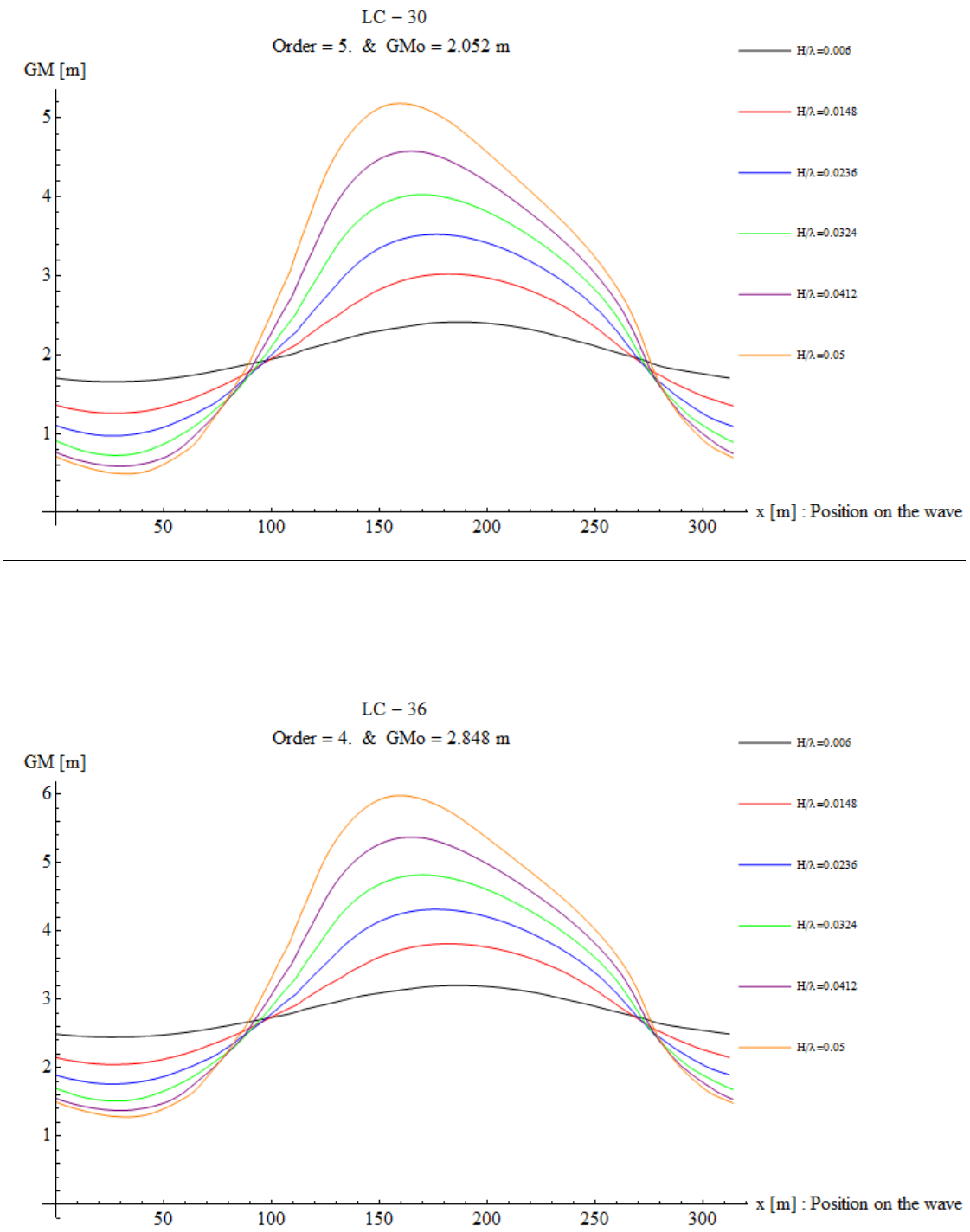

Figure 8.1: GM variations along the wavelength, for a given loading case and wave order and for different values of wave steepness.

As expected, the values of metacentric height tend to increase when the wave steepness or else the wave height increases too. We also observe that the variations become much more intense when the wave height becomes greater. This is a first indication that

parametric roll resonance will occur more easily in higher wave heights. In addition, in LC 15 we observe that in the begging as well as in the ending of the GM variation, the metacentric height becomes of negative value. This happens due to the fact that the initial metacentric height GM_o is quite small in this case. This might also be a clue that the containership model will be more prone to parametric resonance, as a result of the reduced initial stability.

8.2.2. COMPARISON BY WAVE ORDER

Consequently, we are going to compare the variation of GM between the wave orders, from one to five. An indicative diagram for every loading case that corresponds to a specific wave height is presented in figure 8.2.

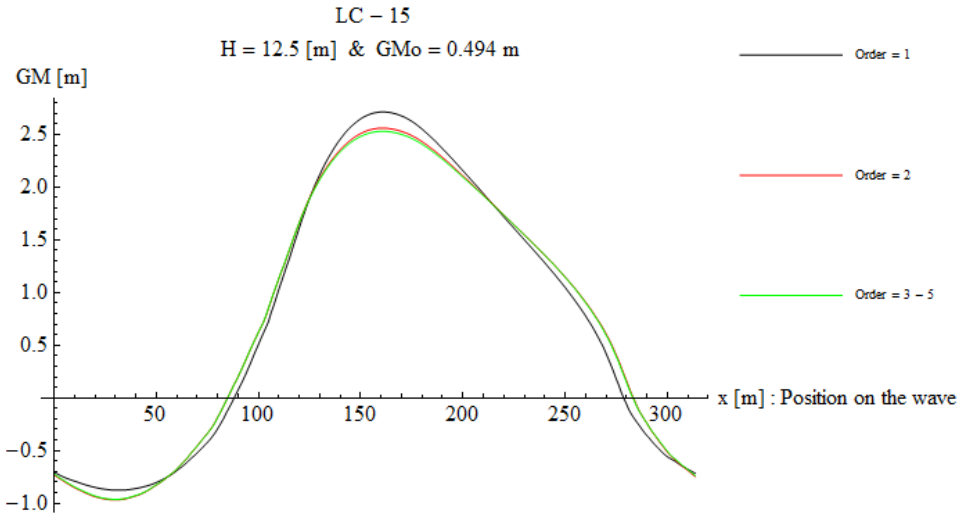

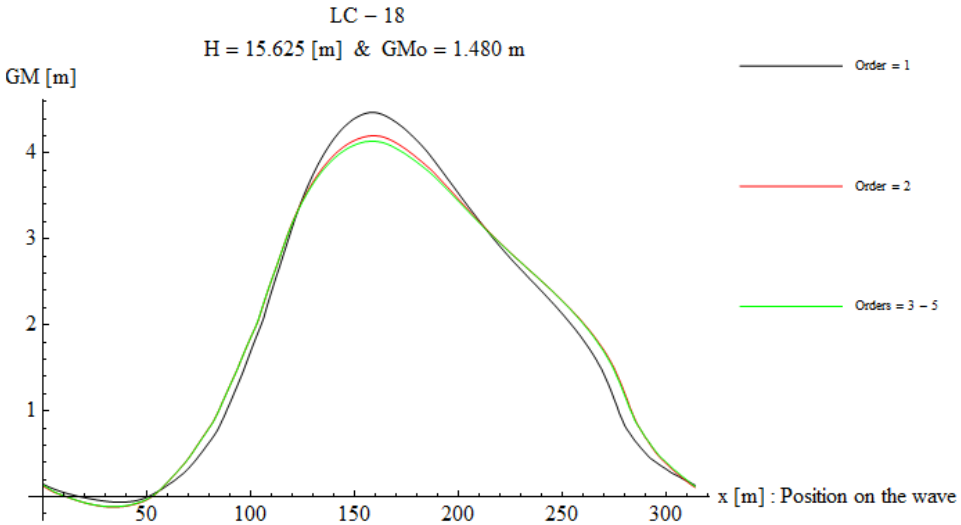

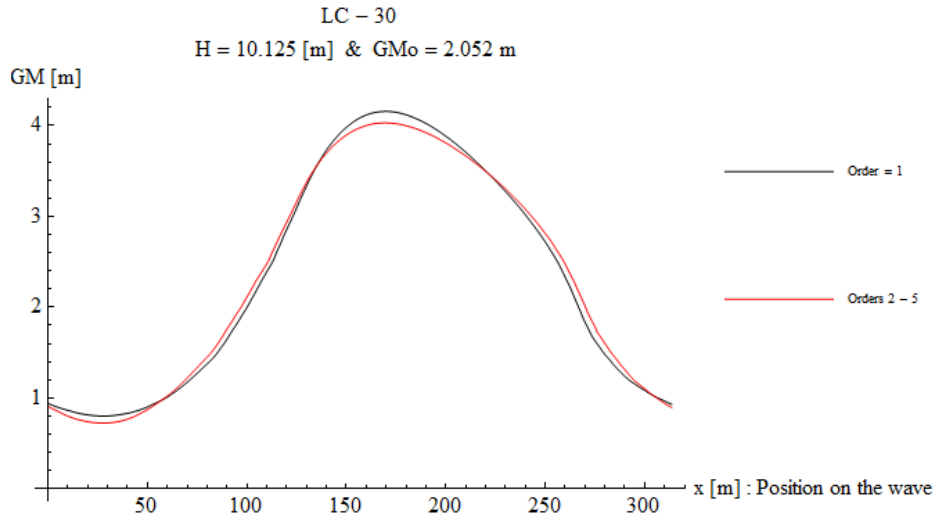

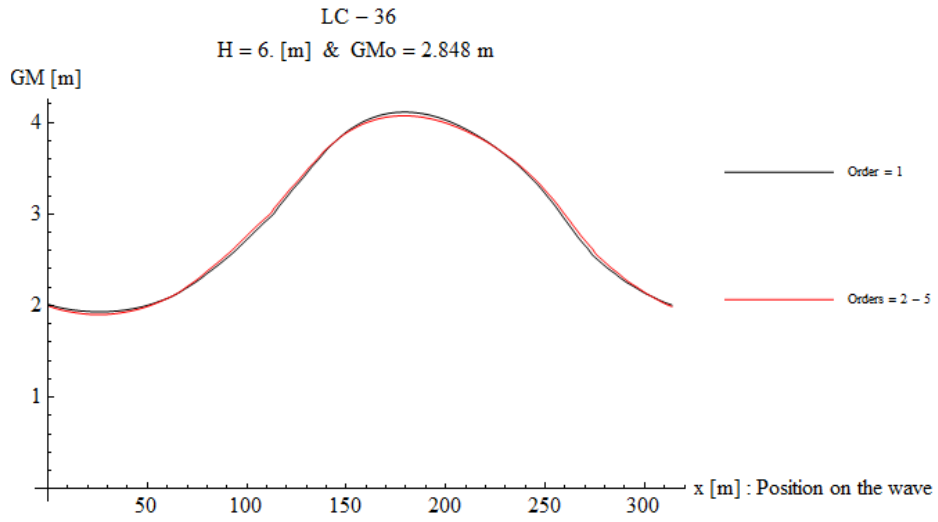

Figure 8.2: Alteration of metacentric height along one wavelength, for a specific wave height and for different wave orders.

Observation of the above diagrams leads to the following conclusion: The divergence between the wave orders intensifies when the wave heights are quite high, as in the case of LC – 15 and LC – 18. In addition, this divergence concerns only the first order, or else linear waves, in comparison to all higher orders (from two to five). With exception of the diagram for LC – 18, where the curve corresponding to the second order wave is slightly deviant to the ones corresponding to the higher orders, all variations for Stokes wave orders two to five are identical. Consequently, proceeding to the creation of the stability charts, we need only to apply the required methodology two wave orders: the first and whichever or the rest four.

8.3. STABILITY CHARTS

Finally, we are now able to move towards the construction of stability charts for parametric roll resonance, by applying the methodology presented in chapter 7. At first, a comparison of between the results obtained with application of two different time-domains is presented in the following figure. The first case corresponds to the solution of the differential roll equation in almost infinite time, considering that a hundred waves have encountered the ship. The second case is more realistic approach, where height cycles are considered.

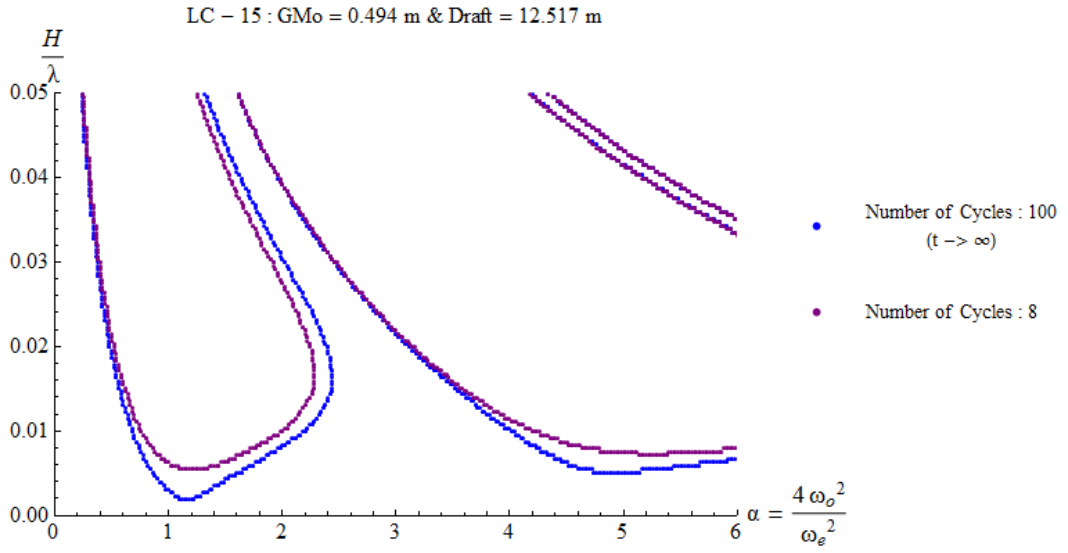

Figure 8.3: Limits of unstable regions when the differential roll equation has been solved for an infinite time-domain (blue) and for eight cycles (purple) of encounter waves.

Though the difference between the two numbers of cycles - 8 and 100- is quite large, the divergence between the corresponding curves in the charts is not proportional to this difference. It seems that most exceeding values of roll amplitude for the unstable pairs of (α,H/λ) are reached quite quickly. We also observe that the minimum wave height for the development of resonance when infinite time has been given to the roll equation is incredibly low (~ 0.6 m), as if there is no damping at all. However, this case is an extreme case with no realistic background.

Subsequently, we are going to investigate the effect of the draft to the response of the containership in parametric roll. The loading condition LC-30 is investigated for both its real draft in design and the draft in scantling, while the initial metacentric height (GM_o), as well as the vertical distance of centroid (KG), remain the same for both cases.

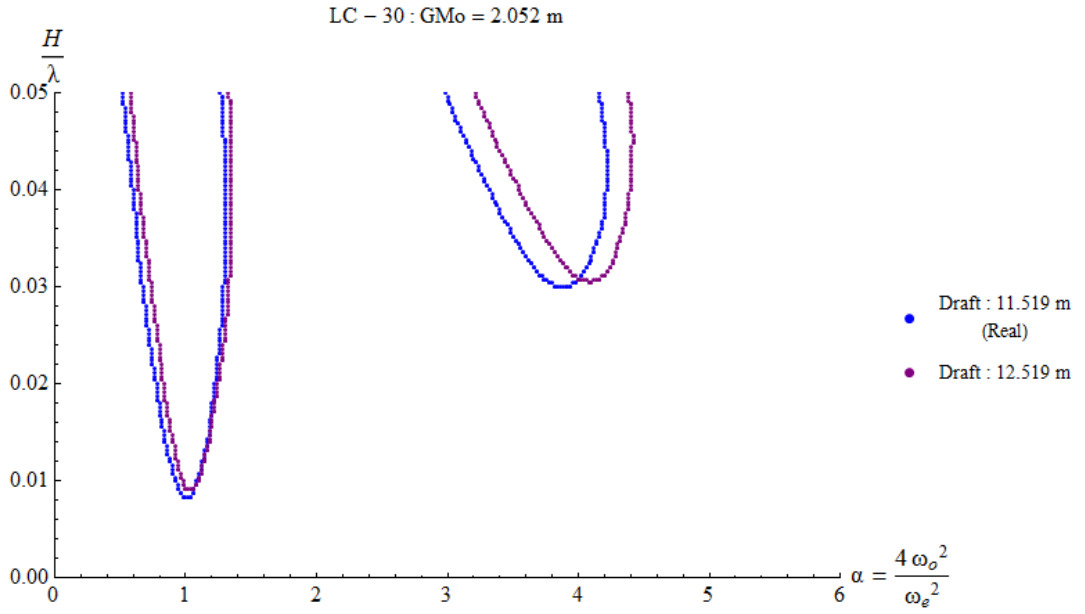

Figure 8.4.: Influence of draft to the limits of unstable regions.

While the first region of instability-around α being equal to one-does not change significantly, the second region of instability-around α being equal to four, seems to be subjected to a parallel transfer towards the right of the horizontal axis when the higher draft is considered. Since the horizontal axisα is directly connected to the ship's forward speed, increment of draft results to the development of parametric resonance in higher speeds than before.

8.3.1. INFLUENCE OF WAVE ORDER

As discussed in the previous subchapter 8.2.2., Stokes wave orders from two to five have the almost the same impact on the fluctuation of the metacentric height. As we have explained in the chapter of the Stoke wave theory (chapter 4.3), the wave celerity is expressed in terms of hyperbolic expressions, with respect to the wave order. In particular, the expression of the wave celerity is given by three different expressions that correspond to:

- 1st expression : 1st and 2nd Wave Order
- 2nd expression : 3rd and 4rth Wave Order
- 3rd expression : 5th Wave Order

In addition, the 2nd and the 3rd expressions are functions of a parameter that is proportional to wave height. Consequently, we choose to examine the cases of first and third wave order, while the latter is the turning point where the wave celerity changes from constant to wave height-varying. For the same reason we should also examine the fifth wave order, but the divergence between the second and third expression for the celerity is infinitesimal.

Subsequently, stability charts for parametric roll resonance are presented, for three loading conditions and for both linear (first order) and irregular (third order) waves.

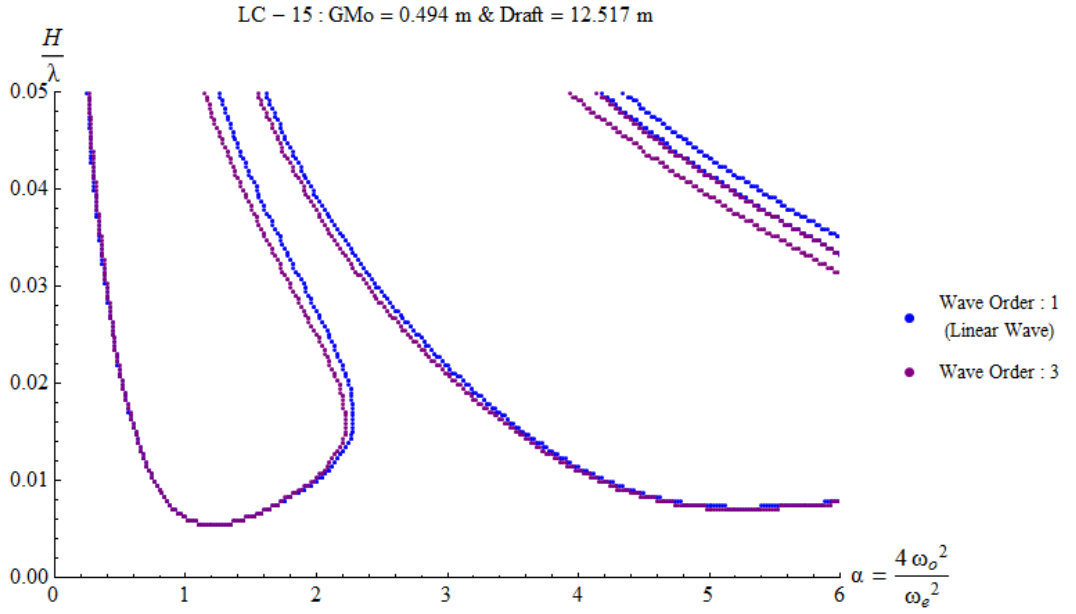

Figure 8.5 : Stability charts for the first and third Stokes wave order, for the loading case LC - 15.

The loading case LC -15 corresponds to a quite low value of initial metacentri height, GM_o=0.494 m. This is propably the reason for the expansion of the instability regions. The fisrt region becomes norrower in the case of the third order wave, while the second region becomes a bit wider. Therefore, it seems that watever loss occurs in the first regions, suchever gain happens in the second. If we define as A_1 and A_3 the whole area of instability respectively for the first and the third wave order, we can calculate the percentage difference as follows:

$$difference = \frac{(A_1 - A_3)}{A_1} 100\% = 0.89\%$$

This means that the third wave order contributed to the reduction of parametric roll resonance development, at 0.89%

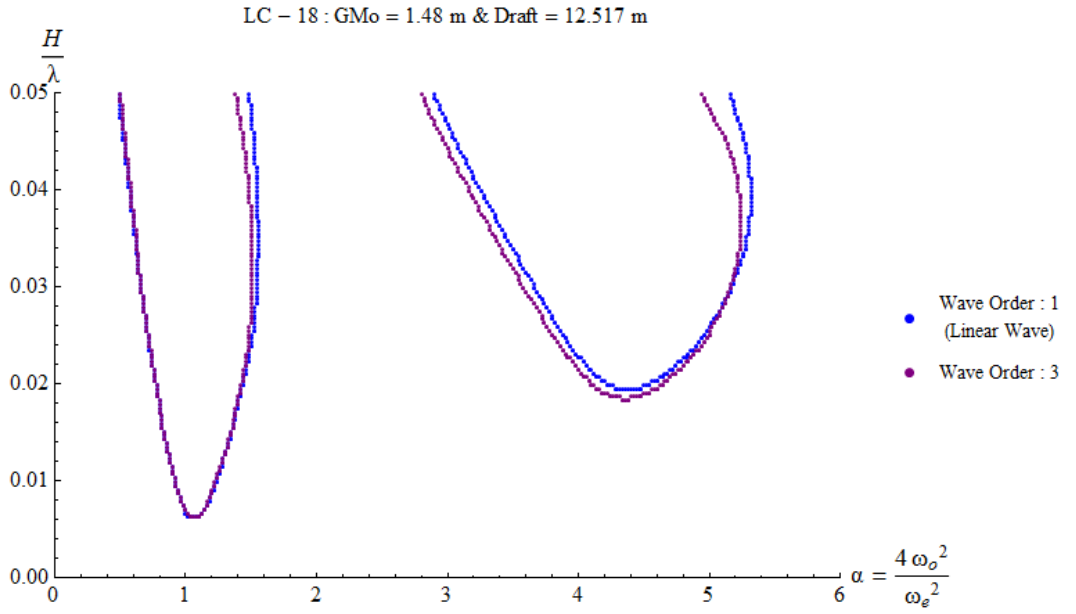

Figure 8.6 : Stability charts for the first and third Stokes wave order, for the loading case LC - 18.

In loading case LC – 18, the instability regions have become significantly narrower, in comparison to the previous case. Here, the initial metacentric height is almost three times that of LC – 15. Here, the percentage difference of the instability regions between the two cases is 0.38%.

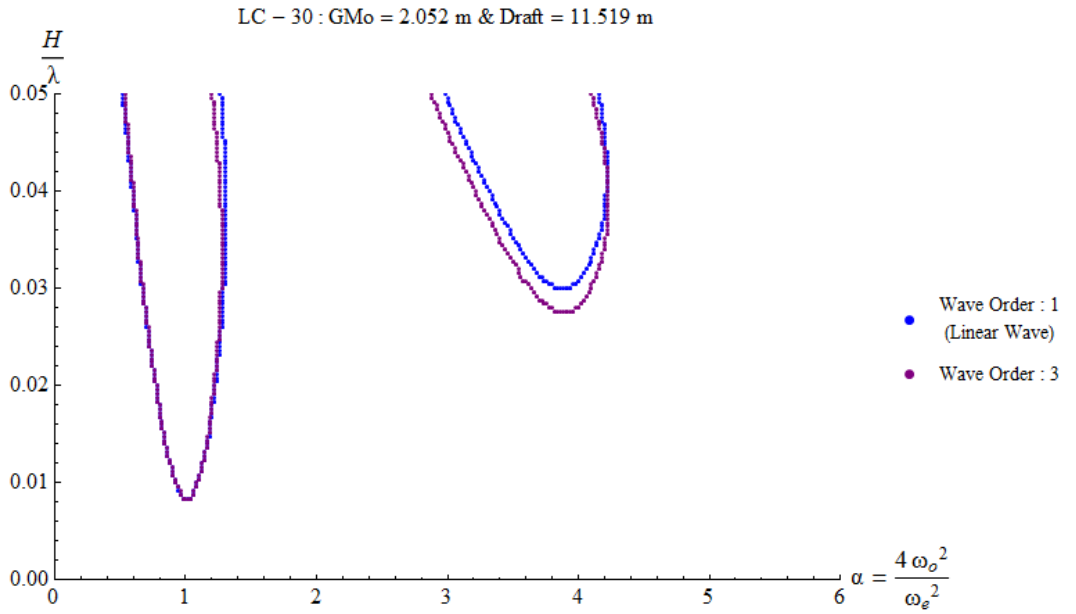

Figure 8.7 : Stability charts for the first and third Stokes wave order, for the loading case LC - 30.

In loading case LC – 30, the area of the instability regions has been subjected to even more loss, in comparison to the previous case. It seems that while the initial metacentric height (GM_o) increases, the ship is less prone to experience severe parametric resonance. Here, the percentage differences rises up to 5.5%. In other words, the irregularity in the wave form is beneficial to the impediment of parametric resonance at 5.5%

8.3.2. INFLUENCE OF SHIP'S FORWARD SPEED

In the current section, the influence of ship's forward speed in the development of parametric roll resonance will be investigated. For these purpose, four regions of speed are considered:

Region of Speed	U [kn]
Super Slow Steaming	< 15
Extra Slow Steaming	15 - 18
Slow Steaming	18 - 21
Full Speed	21 - 24
Unacceptable	> 24

Table 8.2: Table of ship's forward speed regions.

Then, stability charts for the three loading conditions are recreated and presented.

- *LC -15 , GM_o = 0.494 m*

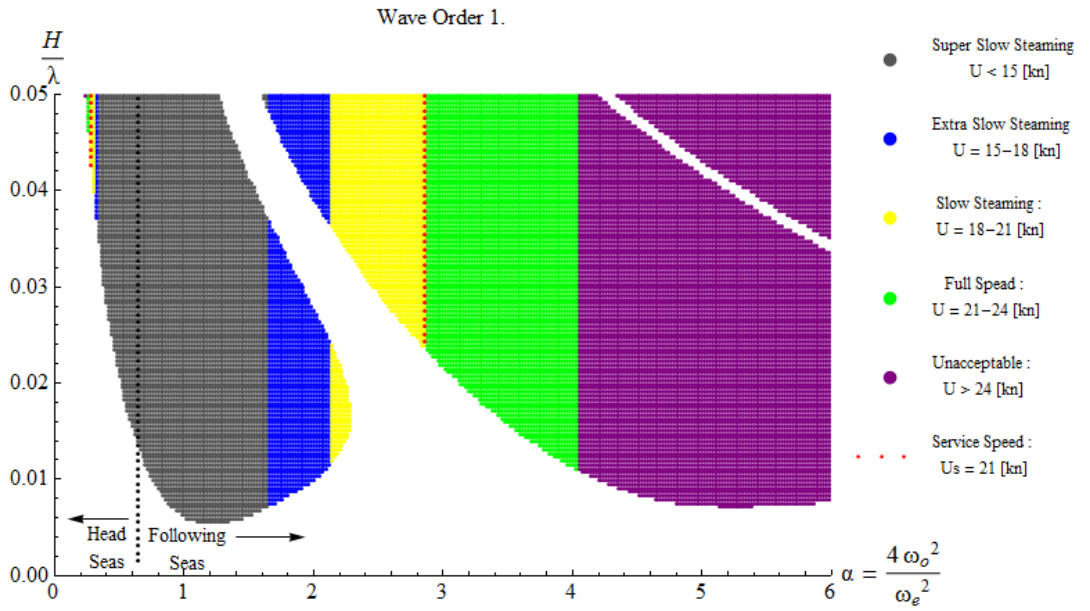

Figure 8.8.: Influence of ship's forward speed on stability charts for LC -15 and for regular waves.

In the above figure 8.8, the black dotted line separates the area of head seas from the area of following seas. The red dotted line represents the service speed of the containership model used in the simulations. The minimum value of wave steepness for which parametric instability arises when the containership is travelling in the service speed U_s=21 [kn] is

- For Head Seas : $(H/\lambda)_{min}$ = 0.0427 => H_{min} = 13.34 m
- For Following Seas : $(H/\lambda)_{min}$ = 0.0259 => H_{min} = 8.09 m

Similarly, for the irregular waves we present:

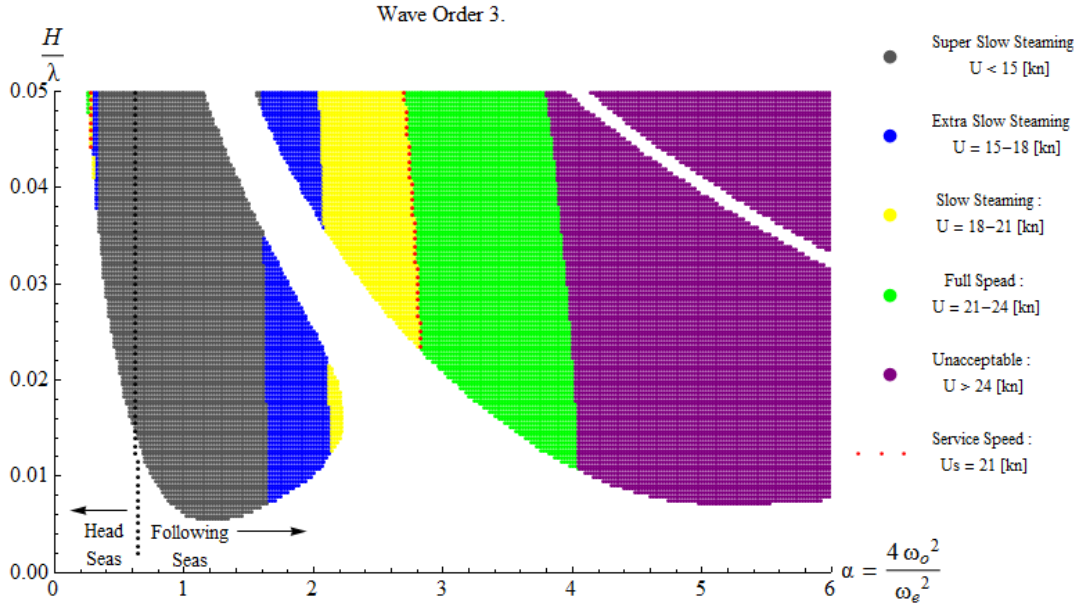

Figure 8.9: Influence of ship's forward speed on stability charts for LC -15 and for irregular waves.

As expected, due to the wave height-varying nature of the wave celerity, the limits of the speed regions are not constant along the vertical axis. If we calculate again the minimum required value of wave height for parametric instability in the service speed, we get:

- For Head Seas : $(H/\lambda)_{min}$ = 0.0443 => H_{min} = 13.84 m
- For Following Seas : $(H/\lambda)_{min}$ = 0.0259 => H_{min} = 8.09 m

Afterwards, we calculate the percentage differences of the instability areas between those corresponding to regular waves and those concerning irregular, for each region of speed individually, as shown in the following table 8.3.

Region Of Speed	Percentage Difference (%) Of order 3 to 1
Super Slow Steaming	-3.99
Extra Slow Steaming	-7.49
Slow Steaming	-7.72
Full Speed	-2.79
Unacceptable	+4.4

Table 8.3: Percentage differences of the speed /instability regions between the cases of regular and irregular seas, for LC -15.

We note that negative sign (-) in the percentage difference indicates that the third wave order contributes negatively to the expansion of the speed/instability region. Respectively, the positive sign means that the nonlinearity helps the speed/instability region to increase. In the current loading case, we conclude that for a forward speed under 24 [kn], the ship is less likely to experience parametric resonance when the encounter waves are irregular than when they are regular. This response intensifies in the region of Extra Slow Steaming and Slow Steaming.

The same investigation is applied to the remaining loading conditions, as follows:

- *LC -18, GM_o = 1.480 m*

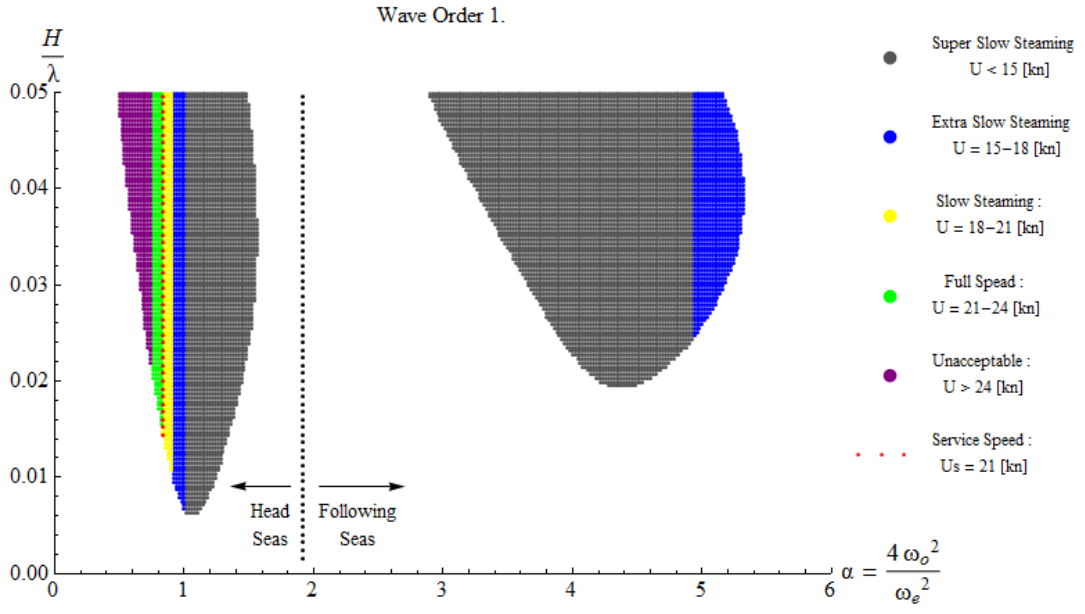

Figure 8.10: Influence of ship's forward speed on stability charts for LC -18 and for regular waves

The minimum required value of wave height for parametric instability in the service speed is (only for head seas):

$(H/\lambda)_{min}$ = 0.0144 => H_{min} = 4.5 m

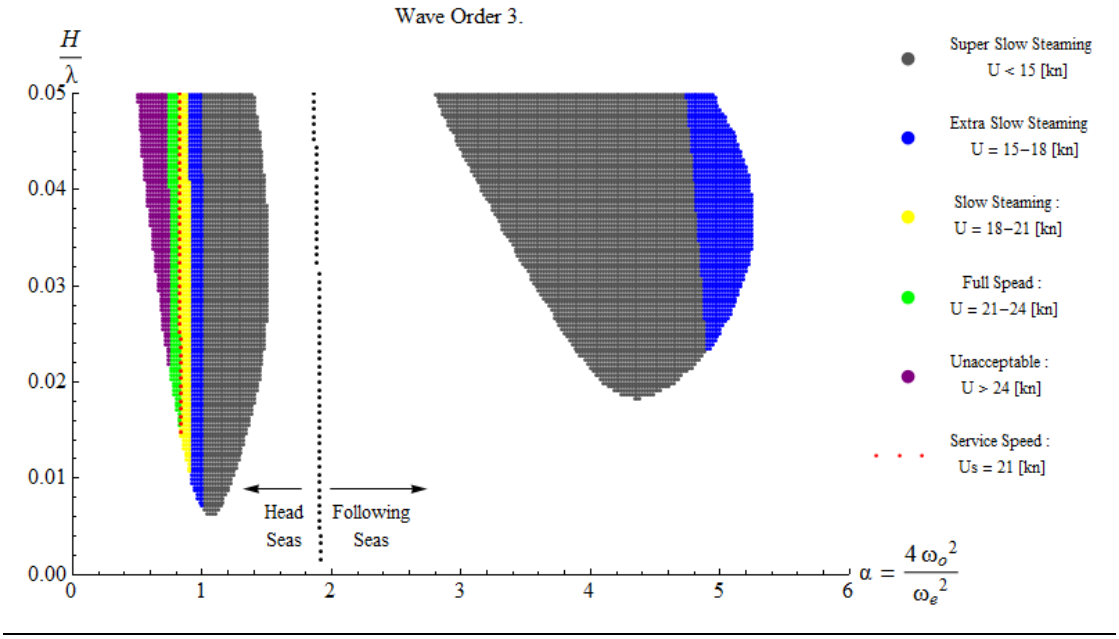

Figure 8.11: Influence of ship's forward speed on stability charts for LC -18 and for irregular waves

The minimum required value of wave height for parametric instability in the service speed is (only for head seas):

$(H/\lambda)_{min}$ = 0.0148 => H_{min} = 4.625 m

Region Of Speed	Percentage Difference (%) Of order 3 to 1
Super Slow Steaming	-1.60
Extra Slow Steaming	+7.80
Slow Steaming	+9.57
Full Speed	-11.73
Unacceptable	-7.74

Table 8.4: Percentage differences of the speed /instability regions between the cases of regular and irregular seas, for LC -18.

In this loading condition, in contrary to the LC – 15, the nonlinearity of the waves contributes to the speed regions of Extra and Slow Steaming of becoming more dangerous for the occurrence of parametric roll resonance. In addition, the region of higher speeds (Full Speed: 21-24 [kn]) should be preferred when the encounter waves are irregular.

- *LC -30, GM_o = 2.052 m*

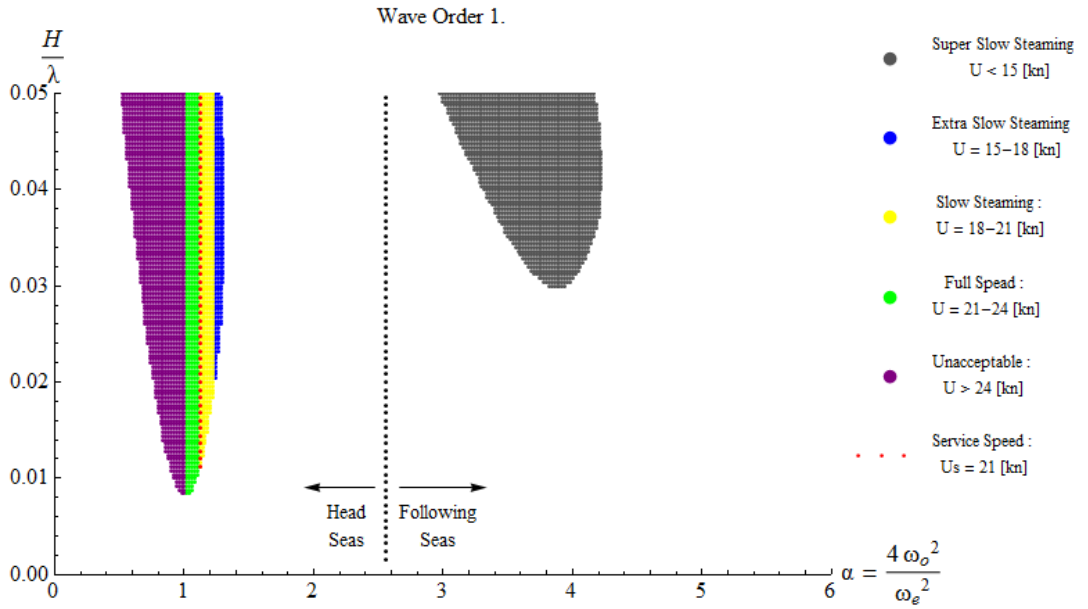

Figure 8.12.: Influence of ship's forward speed on stability charts for LC -30 and for regular waves.

The minimum required value of wave height for parametric instability in the service speed is (only for head seas):

$(H/\lambda)_{min}$ = 0.0112 => H_{min} = 3.50 m

For the irregular waves:

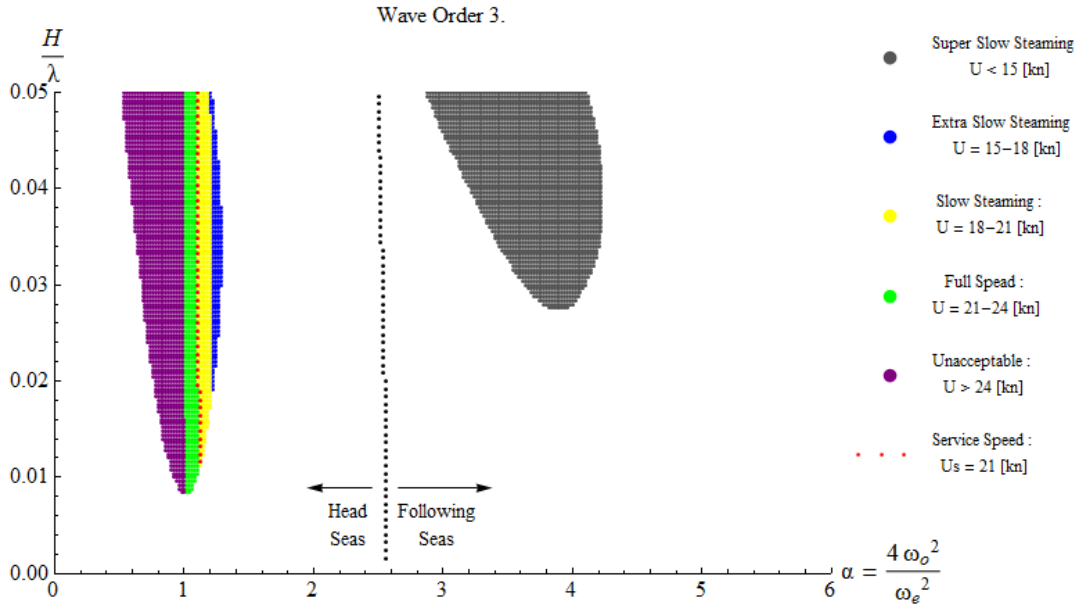

Figure 8.13.: Influence of ship's forward speed on stability charts for LC -30 and for irregular waves.

The minimum required value of wave height for parametric instability in the service speed is (only for head seas):

$(H/\lambda)_{min}$ = 0.0116 => H_{min} = 3.625 m

Region Of Speed	Percentage Difference (%) Of order 3 to 1
Super Slow Steaming	+16.78
Extra Slow Steaming	-12.45
Slow Steaming	-2.04
Full Speed	+1.53
Unacceptable	-6.01

Table 8.5: Percentage differences of the speed /instability regions between the cases of regular and irregular seas, for LC -30.

In the current loading condition, the nonlinearity of the waves contributes to the speed region of Extra Slow Seaming of becoming much less dangerous for the occurrence of parametric roll resonance. In addition, the region of Super Slow Steaming should be avoided when the encounter waves are irregular.

Next, the stability chart for the last loading condition LC – 36 is presented:

- *LC – 36, GM_o = 2.848 m*

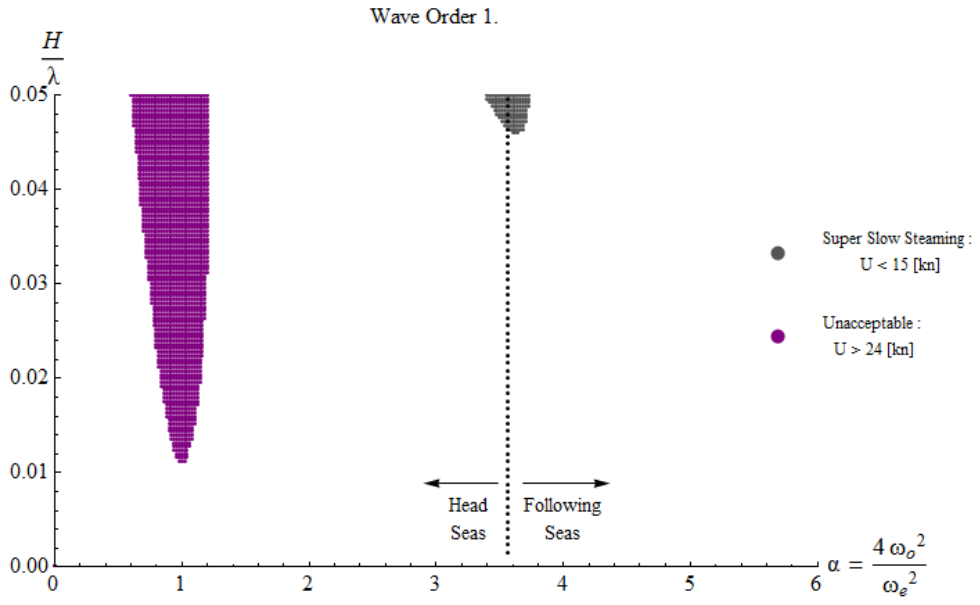

Figure 8.14: Stability chart for LC – 36, for regular seas and with influence of ship's forward speed.

This case is the safest as far as it concerns the ship's response in parametric roll. As we see, the only significant in range instability region concerns speeds that are considered unacceptable (>24 kn). The second region may correspond to possible values of speed, but it

is incredibly small and it can be considered negligible. In addition, this is the only one of the four loading cases that does not present parametric roll resonance in the service speed. Consequently, there is no need proceeding to calculations for the third order waves.

8.3.3. INFLUENCE OF THE INITIAL METACENTRIC HEIGHT (GM_o)

The loading condition on which the containership is sailing plays as significant role in the development of instability regions. As we have presented in the previous subchapters, while the initial metacentric height grows, the regions of instability become smaller. Therefore, the initial stability is a determinant factor with respect to the overall image of the stability charts. However, when the factor of speed is introduced into the investigation, it is of high interest to examine whether a loading condition with higher initial stability is beneficial to the ship's response in parametric roll, while the vessel travels with its service speed. The following table presents a comparison between the three loading cases considered for the analysis, with respect to the minimum required height H_{min} for parametric instability to occur, in the service speed U_s=21 kn.

Loading Condition	**Initial Metacentric Height GM_o [m]**	**H_{min} [m] for resonance in U_s=21 [kn]**
LC -15	0.494	8.09
LC -18	1.480	4.50
LC-30	2.052	3.50

Table 8.6 : Minimum required have height for parametric resonance in the service speed.

As we observe, while the initial metacentric height grows, a less value of wave height is needed so that the response of the ship enters the region of instability. As a conclusion, a high initial value of metacentric height will help the ship to be less prone of parametric roll resonance in general, but in will be much more vulnerable in its service speed. The issue of predicting instability becomes even more perplexed when we introduce the factor of nonlinearity in the study. In the following table we present the difference of the instability/speed regions for order 3 to order 1, with comparison between the loading cases.

Region Of Speed	**LC -15, GM_o=0.494m**	**LC -18, GM_o=1.480m**	**LC -30, GM_o=2.052m**
	Difference % of Wave Order 3 to 1		
Super Slow Steaming	-3.99	-1.60	+16.78
Extra Slow Steaming	-7.49	+7.80	-12.45
Slow Steaming	-7.72	+9.57	-2.04
Full Speed	-2.79	-11.73	+1.53
Unacceptable	+4.4	-7.74	-6.01

Figure 8.7: Difference between the instability/speed regions in irregular seas to those in regular, for all three loading cases.

As occurs, when the containership travels in LC-15, with the smallest initial metacentric height, the nonlinearity in waves is beneficial for the response of ship in total. All instability/speed regions under 24 kn are reduced, while the region of unacceptable speed (>24 kn), speed that is definitely not expected, is increased. In particular, the regions of Slow Steaming and Extra Slow Steaming are significantly decreased, i.e. these range of speeds should be preferred. In LC -18, with an initial metacentric height almost three times that of LC-15, the speed regions of Extra Slow Steaming and Slow are quite increased, in contrary to the previous case, while Full Speed region is significantly decreased. We can conclude then, that in this case a higher range of speed should be preferred, rather than slow steaming speeds. Finally, in the third case LC-30, we observe that the Super Slow Steaming region is greatly increased when the nonlinearity in waves is considered, while the Slow Steaming is decreased enough. Then, in this case, very low speeds (<15 kn) should not be achieved when irregular waves are encountered.

9. CONCLUSIONS AND FUTURE WORK

9.1 CONCLUSIONS

In the framework of the present thesis, the response of a containership in parametric roll has been investigated. Both following and head seas as well as both regular and irregular seas have been taken into consideration. The study was focused on the creation of stability charts for parametric roll resonance, for four different loading cases of the model containership. For this purpose, a numerical simulation in the environment of MATHEMATICA was created, for the calculation of the exact variation of metacentric height and the construction of the charts. The mathematical model used is a single-degree of freedom in roll, with linear damping and nonlinear restoring, since the exact value of metacentric height is obtained for every position of the ship on the wave.

The analysis of the stability charts was focused on three basic parameters:

- Linearity/Nonlinearity in encounter waves
- Ship's forward speed
- Loading Condition

Since the sea environment is undoubtedly better approached with nonlinear waves, Stokes third order waves were compared to the first order (regular seas), with respect to the ship's response in parametric roll. The horizontal axis of the charts is a function of ship's forward speed, so the influence of the latter to the development of instability regions could easily be examined. In addition, the loading condition selected for the calculations determined the definition of the limits of the instability regions, since the initial value of metacentric height plays a significant role to the fluctuation of the GM(x) curve, where x is the position of the ship on the wave. Finally, we end up to the following conclusions:

- The nonlinearity in waves does not play a very significant role for the stability charts. However, when taking into consideration the ship's forward speed, the nonlinearity may, or may not, be beneficial for certain regions of speed.

- The loading condition of the containership is crucial to the ship's response in parametric roll. Prima facie, the higher the initial metacentric height, the better for the precaution of parametric instability in general. However, for the model containership studied, when the initial metacentric rises, the minimum required wave height for parametric resonance to occur in the ship's service speed gets lower.

- Furthermore, when taking into consideration the ship's forward speed combined with nonlinearity in waves, the selection of the suitable wave speed for prevention of resonance becomes a complicated issue. For nonlinear waves, some regions of speed are more appropriate, in comparison to respective areas for linear waves.

- As a useful guidance on board, results of investigation of parametric roll resonance and associated stability charts for all loading cases should exist.

- Last, we also examined the influence of the draft on the limits of instability regions. As we showed, when the draft increases for a given loading case, not important divergence occurs. Only the second region is objected to a parallel transfer to the right, i.e. higher speeds are required for the introduction into the second region of instability.

9.2 FUTURE WORK

Proposals with respect to the expansion of the work provided by the present thesis are presented, as follows:

- Consideration of a nonlinear model for the differential roll equation and coupling with heave, pitch, or even all six degrees of freedom.

- Consideration of the nonlinear terms of damping.

- A probabilistic approach to the phenomenon of parametric roll, with the sea environment described as a stochastic process or by waves groups. These approaches are closer to the real form of the ocean waves.

- Model experiments for the verification of the analytical and numerical results.

10. REFERENCES

[1] B. Cushman-Roisin, “Part II: Processes, Chapter 4: Waves”, *Course notes, Thayer School of Engineering, Dartmouth College.*

[2] V.L. Belenky and C. Bassler, “Procedures for Early-Stage Naval Ship Design Evaluation of Dynamic Stability: Influence of the Wave Crest”

[3] V. L. Belenky and Sevastianov, “Stability and Safety of Ships”, Second edition 2007.

[4] W. Blocki, “Ship safety in connection with the parametric resonance of the roll,” *International Shipbuilding Progress*, vol. 27, pp. 36–53, 1980.

[5] G. Bulian, “Development of analytical nonlinear models for parametric roll and hydrostatic restoring variations in regular and irregular waves”,*Phd thesis*, 2006.

[6] G. Bulian, A. Francescutto and C. Lugni, “On the nonlinear modeling of parametric rolling in regular and irregular seas*”, 8th International Conference on the Stability of Ships and Ocean Vehicles*, 2003.

[7] S. M. Carmel, “Study of Parametric Rolling Event on a Panamax Container Vessel”, 2006

[8] A. D. D. Craik,”The origins of water wave theory”. *Annual Review of Fluid Mechanics 36: 1–28*, 2004

[9] R. P. Dallinga, J. J. Blok, and H. R. Luth, “Excessive rolling of cruise ships in head and following waves”, *RINA International Conference on ship Motions & Maneuverability*, London, February 1998.

[10] H. Moideen, J.M. Falzarano,“A Critical Assessment of Ship Parametric Roll Analysis”, *Proceedings of the 11th International Ship Stability Workshop*, 2009.

[11] M. Faraday, “On a peculiar class of acoustical figures; and on certain forms assumed by groups of particles upon vibrating elastic surfaces,” *Philosophical Transactions of the Royal Society of London*, vol. 121, pp. 299–340,1831.

[12] J. D. Fenton, “Nonlinear Wave Theories”, *The Sea, Vol.9: Ocean Engineering Science*, 1990.

[13] W. N. France, M. Levandou, T. W. Treakle, J. R. Paulling, R. K. Michel and C. Moore, “An investigation of Head-Sea Parametric Rolling and its Influence on Container Lashing Systems”, *SNAME Annual Meeting Presentation*, 2001.

[14] A. Francescutto, A., D. Dessi and R. Penna, R., “Some Remarks on the Nonlinear Modelling of Parametric Rolling*”, The Eleventh International Offshore and Polar Engineering Conference, 17-22 June, Stavanger, Norway, ISOPE-I-01-280*, 2001.

[15] W. Froude, “On the rolling of ships*,” Transaction of the Institution of Naval Architects, vol. 2, pp. 180–227*, 1861.

[16] R. Galeazzi, “Autonomous Supervision and Control of Parametric Roll Resonance”, *PhD thesis*, October 2009.

[17] H. E. Krogstad and O. A. Arntsen, “Linear Wave Theory”, *Course Notes, Part A, Regular Waves,* February 2000.

[18] ITTC, “Report of the Stability in Waves Committee”, *Proceedings 24th International Towing Tank Conference, 40pp*, 2005.

[19] J. E. Kerwin, “Notes on rolling in longitudinal waves,” *International Shipbuilding Progress, vol. 2(16), pp. 597–614*, 1955

[20] H. R. Luth and R. P. Dallinga, “Prediction of excessive rolling of cruise vessels in head waves and following waves”, *PRADS Conference, The Hague Netherlands*, 1998

[21] M. Levadou, G. Gaillarde, “Operational Guidance to avoid parametric roll”, 2004.

[22] MaxSurf, “Formation Design Systems, User Manual”, 2013.

[23] J. R. Paulling and R. M. Rosenberg, “On unstable ship motions resulting from nonlinear coupling,” *Journal of Ship Research, vol. 3(1), pp. 36–46*,1959.

[24] J. R. Paulling,”Parametric Rolling of Ships, Then and Now”, *Contemporary Ideas on Ship Stability and Capsizing in Waves Fluid Mechanics and Its Applications, vol. 97, pp 347-360,* 2011.

[25]S.Y.Hong,H.C.Yu,S.Kim,H.G.Sung,“Investigationofparametricrollofacontainershipnirregularseasbynumerical simulation”, *10th International Conference on Stability of Ships and Ocean Vehicles,* 2009.

[26]G. Scanferla, “Development of a computational procedure for the derivation of boundaries of parametric roll in a longitudinal seaway*”, Final Year Thesis Erasmus/Socrates Exchange from the University of Trieste to the National Technical University of Athens,* 2006.

[27] D. Spanos and A. Papanikolaou, “Benchmark Study on Numerical Simulation Methods for the Prediction of Parametric Roll of Ships in Waves”, *Proceedings of the 10th International Conference on Stability of Ships and Ocean Vehicles*, 2009.

[28] Y. S. Shin, V. L. Belenky, R. J. Paulling, K. M. Weems and W.M. Li ,“Criteria for Parametric Roll of Large Containerships in Longitudinal Seas”, *ABS Technical Paper*, 2004.

[29] K.J. Spyrou, “Design Criteria for parametric rolling”,*Oceanic Engineering International, Vol. 9, No. 1, 2005, pp. 11-2*, 2005.

[30] K.J. Spyrou, “Design Against parametric Instability in following seas”,*Ocean Engineering 27 625–653*, 2000.

[31] K.J. Spyrou , I. Tigkas, G. Scanferla, N. Pallikaropoulos, N. Themelis, “Prediction potential of the parametric rolling behavior of a post-panamax containership”, *Ocean Engineering,* 2008

[32] C. Archer et al., “Chapter 1 Dynamical Models of Extreme Rolling of Vessels in Head Waves”, *Proceedings of the 67th European Study Group Mathematics with Industry*.

[33] N. Umeda, H. Hashimoto, D. Vassalos, S. Urano and K. Okou, “Nonlinear dynamicsonparametric roll resonancewith realistic numerical modeling”, *8th International Conference on the Stability of Ships and Ocean Vehicles*, 2003.

[34] Ι. Κοντολέφας, “Αριθμητική μελέτη του φαινομένου Surf-Riding σε ακολουθούντες κυματισμούς ανωτέρας τάξης”, *διπλωματική εργασία*, 2012.

[35] Κ. Σπύρου, “Ευστάθεια Διατοιχισμού Πλοίου και Υπόβαθρο Κανονισμών”, *Σημειώσεις Μαθήματος*, 2006.

[36] S. Chakraborty, ”The physics behind parametric roll”, *article in http://lshipdesign.blogspot.gr*, April 2014.

[37] http://www.cargolaw.com

[38] http://www.dnv.no

[39] http://www.usna.edu.

[40] IMO-MSC/Circ. 707: Guidance to the master for avoiding dangerous situations in following and quartering seas, October 1995.

[41] A. R. J. M. Lloyd, “Seakeeping ship behavior in rough weather”, *Ellis Horwood Series in Marine Technology.*